



Sudan University for Science and Technology
College of Graduate Studies



Assessment of Radiation Dose and Image Quality in Computed Tomography

تقييم الجرعة الإشعاعية وجودة الصورة في التصوير بالأشعة المقطعية

*A thesis submitted for fulfillment of the requirements of PhD degree in
Medical Physics*

By:

Badria HbeebAlla Mohammed Elhassan

Supervisor:

Prof. Mohammed Elfadil Mohamed

Co-supervisor:

Dr. Asmaa Ebrahim Alameen

2019

الآية

قَالَ تَعَالَى:

﴿ قَالَ يَقَوْمِ أَرَأَيْتُمْ إِنْ كُنْتُ عَلَىٰ بَيْنَةٍ مِّن رَّبِّي وَرَزَقَنِي مِنْهُ رِزْقًا
حَسَنًا وَمَا أُرِيدُ أَنْ أُخَالِفَكُمْ إِلَىٰ مَا أَنهَكُم عَنْهُ إِنْ أُرِيدُ إِلَّا
الْإِصْلَاحَ مَا اسْتَطَعْتُ وَمَا تَوْفِيقِي إِلَّا بِاللَّهِ عَلَيْهِ تَوَكَّلْتُ وَإِلَيْهِ أُنِيبُ ﴾ (٨٨)

صدق الله العظيم
سورة هود (88)

Dedication

To :

The soul of my parents..

My beautiful family ..

My teachers ..

My friends ...

Acknowledgements

**I would like to express my appreciation to my supervisor:
Prof. Mohammed Elfadil Mohamed
and very grateful to the family of radiology college for the
encouragement and moral support.**

List of contents

No	Contents	Page
	الإية	I
	Dedication	II
	Acknowledgements	III
	Contents	IV
	List of tables	VIII
	List of figures	XI
	Abstract [English]	XII
	Abstract [Arabic]	XIII
	Chapter one: Introduction	
1.1	Introduction	1
1.2	Medical use of CT	2
1.3	Radiation dose units	3
1.4	CT Image Quality	4
1.4.1	CT Image Contrast	4
1.4.2	Image Noise	5
1.4.3	Signal-to-noise ratio	8
1.5	Problem of The study	8
1.6	Objectives	9
1.7	Significance of the study	9
1.8	Overview of the study	9
	Chapter two Background and Literature Review	
2.1	CT Machine	10
2.1.1	The CT scanner components	10
2.2	CT Generations	11
2.2.1	First-Generation CT Scanners	11
2.2.2	Second-Generation CT Scanners	12
2.2.3	Third-Generation CT Scanners	14
2.2.4	Fourth-Generation CT Scanners	16
2.3	Principles of Helical CT Scanners	18
2.4	Slip-Ring Technology	18
2.5	Capabilities of Single-Row Detector Helical CT	20
2.6	Multiple-Row Detector Helical CT	21
2.7	CT imaging protocol	26
2.7.1	Parameters	26
2.7.1.1	Tube current	27

2.7.1.2	Tube Voltage	27
2.7.1.3	Rotation Time	28
2.7.1.4	Total Scan Length	28
2.7.1.5	Slice Thickness	28
2.7.1.6	Pitch	29
2.7.1.7	Automatic Exposure Control	30
2.7.2	Protocols	30
2.8	CT Dose and unit	31
2.8.1	Radiation dose units	31
2.8.2	Effective dose	31
2.9.1	Computed tomography dose index (CTDI)	32
2.10	Image quality	35
2.10.1	Contras	35
2.10.2	Resolution	36
2.10 .3	Noise	36
2.11	Previous studies	38
	Chapter three Materialand Method	
3.1	Material	44
3.2	design of the study	44
3.3	Population of the study	44
3.4	Sample size and type	44
3.5	Method of data collection	45
	Chapter four Results	
4.1	Results	47
	Chapter five Discussion, Conclusion and Recommendation	
5.1	Discussion	58
5.2	Conclusion	61
5.3	Recommendations	62
	References	63

List of Figures

No.	Description	Page
(1.1)	Modern CT scanner	3
(2.1)	CT scanner	11
(2.2)	Diagram of the first-generation CT scanner	12
(2.3)	Diagram of the second-generation CT scanner	14
(2.4)	Diagram of the third-generation CT scanner	15
(2.5)	Diagram of the fourth-generation CT scanner	17
(2.6)	Principles of helical CT	18
(2.7)	Diagram of the slip-ring configuration	19
(2.8)	Time line of the key technological developments in CT	20
(2.9)	Diagram shows the difference between single-row detector and multiple-row detector CT designs	22
(2.10)	Various detector array designs used in multiple-row detector CTScanners	23
(2.11)	Single CT detector versus Multi slice CT detector	25
(2.12)	Simple overview of a third generation CT-imaging system	26
(2.13)	The effect of pitch on irradiated area	30
(2.14)	Illustrates meaning of the term: CTDI	33
(4.1)	Bar graph show the mean effective dose of the three hospitals	48
(4.2)	Bar graph show mean SSDE in the three hospitals	49
(4.4)	Bar graph shows mean effective dose (in mGy) for every exam type	50
(4.5)	Bar graph shows mean SSDE (in mGy) in the three hospitals	51
(4.6)	Pie graph shows the relative percentage of mean SSDE (in mGy) in the three	52
(4.7)	Scatter plot show a direct linear relationship between noise before the enhancement and after enhancement (A) in the high intensity area and (B) low intensity area	53
(4.8)	Scatter plot show a direct linear relationship between signal before the enhancement and after enhancement (A) in the high intensity area and (B) low intensity area	54
(4.9)	Scatter plot show a direct linear relationship between signal to noise before the enhancement and after enhancement (A) in the high intensity area and (B) low intensity area	55
(4.10)	Scatter plot show a direct linear relationship between contrast before the enhancement and after enhancement	56

List of Tables

No.	Description	Page
(3.1)	CT machines were used to collect data during this study	44
(4.1)	The overall mean of CTDvol, DLP and SSDE values for the three Hospitals	47
(4.2)	The mean values of CTDvol, DLP and SSDE values for Medical Modern Hospital Centre (MMC)	47
(4.3)	The mean values of CTDvol, DLP and SSDE values for Alzaytona Hospital	47
(4.4)	The mean values of CTDvol, DLP and SSDE values for Sawi Hospital	47
(4.5)	Showed mean effective dose (in mGy) in the three hospitals	48
(4.6)	Showed mean SSDE (in mGy) in the three hospitals	49
(4.7)	Showed mean effective dose (in mGy) for every exam type	50
(4.8)	Showed mean SSDE (in mGy) in the three hospitals	51
(4.9)	Significance paired t-test between the image quality factor before and after enhancement	56
(4.10)	The mean, standard deviation, minim and maximum values for the image quality factors	57

Abstract

This descriptive cross-sectional study aim to assess the radiation dose and image quality in CT in order to explore the potential risk of radiation. This study was conducted on three hospitals during the period from 2015-2019 in Khartoum state .CT machines were used to collect data during this study the manufacture General Electric ,Toshiba and General Electric respectively Detector Type 16,16 and 64 respectively, where the Computed Tomography Dose Index($CTDI_{vol}$) mGy, Dose Length Product(DLP)mGy.cm, Size specific dose estimate ($SSDE$)mGy and effective dose (in mSV) were measured for each hospital representing the scanning of head, chest and abdomen as well the image quality that include noise, signal, signal to noise ratio and contrast in high and low intensity areas in CT scan images for the previous parts before and after image enhancement. The main results of this study showed that the maximum $CTDI_{vol}$ was to the head 60.5mGy, the highest DLP was for the abdomen 2121.45mGy.cm, to SSDE was 61.71(mGy) for head as well as the effective dose which is equal to 5.65mSV.also the study showed that the image quality in the body areas of high intensity and low intensity before and after the image enhancement is associated with linear relation as the recession coefficients could be used to estimate the values of image enhancement before processing in order to find out the image quality ,and possibility of using the method to decide the best method of image enhancement. The study conclude that, The Effective dose is higher in hospital3 than other hospitals and SSDE dose is higher in hospital2 than other hospitals. And evaluated effective dose in every Exam type is higher brain than other exams, and the following linear equation can be used to estimate the validity of enhancement before the process which as signal after enhancement (High intensity area) = $(1.31 \times$

Signal) - 64.5, noise after enhancement (Low intensity area) = $(0.824 \times \text{noise}) + 0.278$ and Signal to noise ratio after enhancement (HIA) = $(1.07 \times \text{SNR}) - 3.4$. Contrast after enhancement = $(0.853 \times \text{contrast}) + 16.7$.

This study recommended that CT scan examination for any patient must be justified, QC program are essential to evaluate the patients dose and machine accurate performance, Future studies can be done in order to optimize the radiation dose to establish national diagnostic reference level in Sudan and Application of QC program as a routine task in all x-ray department in order to detect possible future problems.

الخلاصة

هذه دراسة وصفية تحليلية هدفت الى تقويم الجرعة الإشعاعية وجودة الصورة في الأشعة المقطعية حتى يتم اكتشاف الخطر المحتمل للإشعاع . وحسب ما هو معروف في الدراسات أن هناك موازنة بين زيادة الجرعة الإشعاعية لتحسين الصورة وتقليل الجرعة للمريض .

إجراء هذه الدراسة في ثلاثة مستشفيات في ولاية الخرطوم خلال الفترة مابين 2015- 2019 تم قياس مؤشر الجرعة للأشعة المقطعية (mGy) $CTDI_{1}$ ، الجرعة الكلية الناتجة $DLP(mGy.cm)$ ، وتقدير الجرعة الخاصة بالحجم $SSDE (mGy)$ الجرعة الفعالة $ED (mSv)$ ، لكل مستشفى وتم قياسها في الجسم في منطقة الرأس والبطن والصدر بالإضافة الى جودة الصورة بما في ذلك الضوضاء والإشارة ونسبة الضوضاء الى الإشارة والتباين في مناطق الجسم ذات الكثافة العالية والمنخفضة في صورة الأشعة المقطعية قبل تحسين الصورة وبعد التحسين. أظهرت الدراسة بعض النتائج أهمها ان قيمة مؤشر الجرعة للأشعة المقطعية ($CTDI_{vol}$) بالنسبة للرأس هي $60.5(mGy)$ وأن أعلى قيمة للجرعة الكلية الناتجة (DLP) كانت للبطن $2121.45(mGy.cm)$ وكانت $61.71 (mGy)$ بالنسبة لتقدير الجرعة الخاصة بالحجم ($SSDE$) للرأس أيضا والجرعة الفعالة (ED) للرأس كانت $5.51 (mSv)$. أوضحت الدراسة أنقيم جودة الصورة في مناطق الجسم ذات الكثافة المنخفضة والكثافة العالية قبل تحسين الصورة وبعد التحسين ترتبط بعلاقة خطية حيث أن معاملات الانحسار يمكن إستخدامها لتقدير قيم تحسين الصورة قبل المعالجة لإكتشاف الجودة وإمكانية إستخدام هذه الطريقة من أجل إتخاذ القرار الأفضل للتحسين.

Chapter one

Introduction

1.1 Introduction

A CT scan makes use of computer-processed combinations of many X-ray images taken from different angles to produce cross-sectional (tomographic) images (virtual "slices") of specific areas of a scanned object, allowing the user to see inside the object without cutting. Other terms include computed axial tomography (CAT scan) and computer aided tomography.

Digital geometry processing is used to generate a three-dimensional image of the inside of the object from a large series of two-dimensional radiographic images taken around a single axis of rotation(Wikipedia, 2017) Medical imaging is the most common application of X-ray CT. Its cross-sectional images are used for diagnostic and therapeutic purposes in various medical disciplines (Wikipedia, 2017) The rest of this article discusses medical-imaging X-ray CT; industrial applications of X-ray CT are discussed at industrial computed tomography scanning.

The term "computed tomography" (CT) is often used to refer to X-ray CT, because it is the most commonly known form. But, many other types of CT exist, such as positron emission tomography (PET) and single-photon emission computed tomography (SPECT). X-ray tomography is one form of radiography, along with many other forms of tomographic and non-tomographic radiography.

CT produces a volume of data that can be manipulated in order to demonstrate various bodily structures based on their ability to block the X-ray beam. Although, historically, the images generated were in the axial or transverse plane, perpendicular to the long axis of the body, modern scanners allow this volume of data to be reformatted in various planes or even as volumetric (3D)

representations of structures. Although most common in medicine, CT is also used in other fields, such as nondestructive materials testing. Another example is archaeological uses such as imaging the contents of sarcophagi. Individuals responsible for performing CT exams are called radiographers or radiologic technologists(Wikipedia, 2017)Use of CT has increased dramatically over the last two decades in many countries(Wikipedia, 2017)An estimated 72 million scans were performed in the United States in 2007. One study estimated that as many as 0.4% of current cancers in the United States are due to CTs performed in the past and that this may increase to as high as 1.5 to 2% with 2007 rates of CT use however, this estimate is disputed, as there is not a consensus about the existence of damage from low levels of radiation. Side effects from intravenous contrast used in some types of studies include kidney problems. (Wikipedia, 2017)

1-2Medical use of CT

CT has become an important tool in medical imaging to supplement X-rays and medical ultrasonography. It has more recently been used for preventive medicine or screening for disease, for example CT colonography for people with a high risk of colon cancer, or full-motion heart scans for people with high risk of heart disease. A number of institutions offer full-body scans for the general population although this practice goes against the advice and official position of many professional organizations in the field primarily due to the radiation dose applied. (Wikipedia, 2017)



Figure (1.1)Modern CT scanner

1. 3-Radiation dose units

The radiation dose reported in the gray or mGy unit is proportional to the amount of energy that the irradiated body part is expected to absorb, and the physical effect (such as DNA double strand breaks) on the cells' chemical bonds by X-ray radiation is proportional to that energy(Wikipedia, 2017).

The sievert unit is used in the report of the effective dose. The sievert unit, in the context of CT scans, does not correspond to the actual radiation dose that the scanned body part absorbs but to another radiation dose of another scenario, the whole body absorbing the other radiation dose and the other radiation dose being of a magnitude, estimated to have the same probability to induce cancer as the CT scan.(Wikipedia, 2017)Thus, as is shown in the table above, the actual radiation that is absorbed by a scanned body part is often much larger than the effective dose suggests. A specific measure, termed the computed tomography dose index (CTDI), is commonly used as an estimate of the radiation absorbed dose for tissue within the scan region, and is automatically computed by medical CT scanners.(Wikipedia,2017)

The equivalent dose is the effective dose of a case, in which the whole body would actually absorb the same radiation dose, and the Sievert unit is used in its report. In the case of non-uniform radiation, or radiation given to only part

of the body, which is common for CT examinations, using the local equivalent dose alone would overstate the biological risks to the entire organism.

1.4- CT Image Quality

Fundamentally, image quality in CT, as in all medical imaging, depends on many factors the four basic one includes: image contrast, spatial resolution, image noise, and artifacts. Depending on the diagnostic task, these factors interact to determine sensitivity (the ability to perceive low-contrast structures) and the visibility of details.

1.4-1CT Image Contrast

CT image contrast depends on subject contrast and display contrast. Because CT display contrast is arbitrary (depending only on the window level and width selected), it will not be discussed further.

As in radiography, CT subject contrast is determined by differential attenuation: that is, differences in x-ray attenuation by absorption or scattering in different types of tissue and thus resulting in differences in the intensity of the x-rays ultimately reaching the detectors. Because of the high peak kilovoltage and relatively high beam filtration (beam hardness) used in CT, the x-ray/tissue interactions (except in bone) are overwhelmingly Compton-scattering events. Differential attenuation for Compton scatter arises from differences in tissue electron density (electrons/cm³), which in turn are due primarily to differences in physical density (Seibert JAetal,2005). Thus, subject soft-tissue contrast in CT comes mainly from differences in physical density. That the small differences in soft-tissue density can be visualized on CT is due to the nature of the image (a 2-dimensional image of a 2-dimensional slice), the ability to map small attenuation differences to large

differences in gray level by windowing, the near-complete elimination of scatter, and the use of a sufficient x-ray intensity.

Related to CT image contrast is the CT contrast scale. We recall that CT numbers are derived from voxel attenuation coefficients calculated during image reconstruction using the following relationship:

Where μ_p and μ_w are linear attenuation coefficients for a given voxel and for water (μ_w is determined from calibration scans). Because CT number is a linear function of μ_p , a graph of expected CT numbers for materials with known attenuation coefficients should be linear over the clinical CT-number range (e.g., $-1,000$ to $+1,000$). For evaluation of the contrast scale of a scanner, various CT test phantoms are available that contain materials designed to provide certain CT numbers (e.g., the CT numbers for water, fat, soft tissue, bone, and air) (McColloughCHetal, 2000)

1.4-2 Image Noise

If a graphic cursor is used to display pixel CT numbers in an image of a uniform phantom (e.g., a phantom containing all water), it is seen that the CT numbers are not uniform but rather fluctuate around an average value (which should be approximately 0 for water): Some pixels are 0, some are +1, some +2, some -1 , and so forth. These random fluctuations in the CT number of otherwise uniform materials appear as graininess on CT images. This graininess is the CT analog of—and is of the same nature as—radiographic quantum mottle: It is due to the use of a limited number of photons to form the image (Hounsfield GN,1976- Judy PF,2000).

In radiography, image noise is related to the numbers of x-ray photons contributing to each small area of the image (e.g., to each pixel of a direct digital radiograph). In CT, x-rays contribute to detector measurements and not

to individual pixels. CT image noise is thus associated with the number of x-rays contributing to each detector measurement. To understand how CT technique affects noise, one should imagine how each factor in the technique affects the number of detected x-rays. Examples are as follows:

X-ray tube amperage: Changing the mA value changes the beam intensity—and thus the number of x-rays—proportionally. For example, doubling the mA value will double the beam intensity and the number of x-rays detected by each measurement.

Scan (rotation) time: Changing the scan time changes the duration of each measurement—and thus the number of detected x-rays—proportionally. Because amperage and scan time similarly affect noise and patient dose, they are usually considered together as $\text{mA} \times \text{s}$, or mAs.

Slice thickness: Changing the thickness changes the beam width entering each detector—and thus the number of detected x-rays—approximately proportionally. For example, compared with a slice thickness of 5 mm, a thickness of 10 mm approximately doubles the number of x-rays entering each detector.

Peak kilovolt age: Increasing the peak kilovolt age increases the number of x-rays penetrating the patient and reaching the detectors. Thus, increasing the kilovolt age reduces image noise but can (slightly) reduce subject contrast as well.

Although not affecting the numbers of detected x-rays, a reconstruction filter profoundly affects the appearance of noise in the image: Smooth filters blur the noise, reducing its visual impact, whereas sharp filters enhance the noise. In images of soft tissue, noise is generally more interfering than blur, and smoother filters are preferred. In images of structures with edges and small details, such as bone, blur is generally more interfering than noise, and sharper

filters are preferred. For comparison, Figure 10 shows examples of noise in scans of uniform phantoms using standard and higher-resolution (bone) filters and with standard and very low values for mAs.

Comparison of noise from scans using 270 mAs (typical clinical value) and 100 mAs. (C) Appearance of image noise is strongly affected by reconstruction filter; sharp filter such as bone also sharpens (enhances) appearance of noise.

Because CT noise appears as fluctuations in CT numbers, a measurement of image noise is a measurement of these fluctuations, and such a measurement can be made using regions of interest (ROIs) on a scan of a uniform phantom. A statistical ROI function (available on most CT scanners) allows users to place a rectangular or oval ROI on the image, within which is calculated the average and standard deviation (SD) of the CT numbers for the enclosed pixels. The SD indicates the magnitude of random fluctuations in the CT number and thus is related to noise: The larger the SD, the higher the image noise.

Because noise is the most bothersome when one is viewing low-contrast soft-tissue structures, an important test of scanner performance is how well low-contrast test objects are seen in the presence of typical noise levels. Figure 11 is an example of a low-contrast test phantom, consisting of groups of rods embedded in material producing approximately 0.6% subject contrast (i.e., a nominal CT-number difference of 6 between the rods and the background). The rod groups range in diameter from 6 to 2 mm. In this example, the 5-mm rods are visible, whereas the smaller ones are lost in the noise.

Low-contrast phantom to test CT performance in presence of typical image noise levels (from American College of Radiology accreditation phantom). Five-millimeter rods are visible, but smaller ones are obscured by noise.

Signal-to-noise ratio (abbreviated SNR or S/N) is a measure used in science and engineering that compares the level of a desired signal to the level of background noise. It is defined as the ratio of signal power to the noise power, often expressed in decibels. A ratio higher than 1:1 (greater than 0 dB) indicates more signal than noise. While SNR is commonly quoted for electrical signals, it can be applied to any form of signal (such as isotope levels in an ice core or biochemical signaling between cells).

The signal-to-noise ratio, the bandwidth, and the channel capacity of a communication channel are connected by the Shannon–Hartley theorem.

1.4-4Signal-to-noise ratio

Is sometimes used metaphorically to refer to the ratio of useful information to false or irrelevant data in a conversation or exchange. For example, in online discussion forums and other online communities, off-topic posts and spam are regarded as "noise" that interferes with the "signal" of appropriate discussion.

1.5-Problem of The study

Radiation like X-rays might lead to serious health problem to the practitioners and patient as well if certain measures were not taken seriously, which means potentially the risk exist, therefore it is essential land in fact mandatory to reduce the radiation dose in diagnostic radiology as far as possible at the same time produces a good quality image that reveal the health condition from the first exposure.

1.6-Objectives

The general objective of this study was to assess radiation dose and image quality in CT in order to explore the potential risk and image suitability.

Specific objective

- To estimate patient effective dose in three hospital
- To measure CTDvol, DLP and SSDE values for head, abdomen and chest
- To find signal, noise and signal to noise ratio in high and low intensity areas before and after image enhancement.
- To assess the image contrast before and after enhancement
- To find the significance differences between the image quality factor before and after enhancement.
- To estimate the quality of image enhancement from current quality factor.

1.7-Significance of the study

This study will make it possible to obtain an optimized image ideal for diagnosis of the disease as well as applying the lowest dose to the patient in order to protect the patient while getting the best image quality.

1.8-Overview of the study

The study consisted of five chapters; with Chapter one is an introduction which includes definition of CT scans, medical use, Radiation dose units and Image Quality parameters, as well as the problem of the study, an objective and significance of the study. Similarly Chapter two includes a comprehensive literature review. Chapter three includes the methodology of the study which discussed the material used to collect the data and in the method followed in data acquisition. Chapter four which presented the results and Finally Chapter five which included discussion, conclusion and recommendations of the study.

Chapter Two

Background and Literature Review

2.1 CT Machine

2.1.1 The CT scanner components

The general structure of CT equipment can be divided in three principle elements:

1- The Data Acquisition and Transfer system, which encompasses the gantry, the patient's table, the power distribution unit and the data transfer unit. (Nunes, 2010)

The Gantry which is a central opening gantry is a moveable frame that contains the x-ray tube including collimators and filters, detectors, data acquisition system (DAS), rotational components including slip ring systems and all associated electronics such as gantry angulations motors and positioning laser lights. A CT gantry can be angled up to 30 degrees toward a forward or backward position.

The Table is where the patients is positioned (lie down), and it moves through the gantry. The patient's table and the gantry constitute CT scanner itself.

The power Distribution unit supplies power to the gantry, the patient's table and the computers of the Computing System, which is localized in a separate room as will be explained next.

The computing System(or operator's console) is installed in separate room, making it possible for the operator (technician)to control the acquisition process, introducing patient data and selecting several acquisition parameters such as the kVp , mA values the protocol is going to use (Nunes, 2010). Also there is another operator's console for editing and post-processing is also

necessary, so it possible to analyze and review previous exam data, without interfering with the current examinations taking place.



Figure (2.1) CT scanner

The image reconstruction system: receives the X-ray transmission data information from the data transfer unit, in a digital format. This gathered data is then corrected to using reconstruction algorithms and later stored (Nunes,2010).

2.2 CT Generations

2.2.1 First-Generation CT Scanners

The EMI Mark I scanner, the first commercial scanner invented by Hounsfield, was introduced in 1973 (Hounsfield GN., 1973). This scanner acquired data with an x-ray beam collimated to a narrow “pencil” beam directed to a single detector on the other side of the patient; the detector and the beam were aligned in a scanning frame. A single projection was acquired by moving the tube and detector in a straight-line motion (translation) on opposite sides of the patient (Fig 2.2). To acquire the next projection, the frame rotated 1° , then translated in the other direction. This process of translation and rotation was repeated until 180 projections were obtained. The

earliest versions required about 4.5 minutes for a single scan and thus were restricted to regions where patient motion could be controlled (the head). Since procedures consisted of a series of scans, procedure time was reduced somewhat by using two detectors so that two parallel sections were acquired in one scan. Although the contrast resolution of internal structures was unprecedented, images had poor spatial resolution (on the order of 3 mm for a field of view of 25 cm and 80×80 matrix) and very poor z-axis resolution (13-mm section thickness).

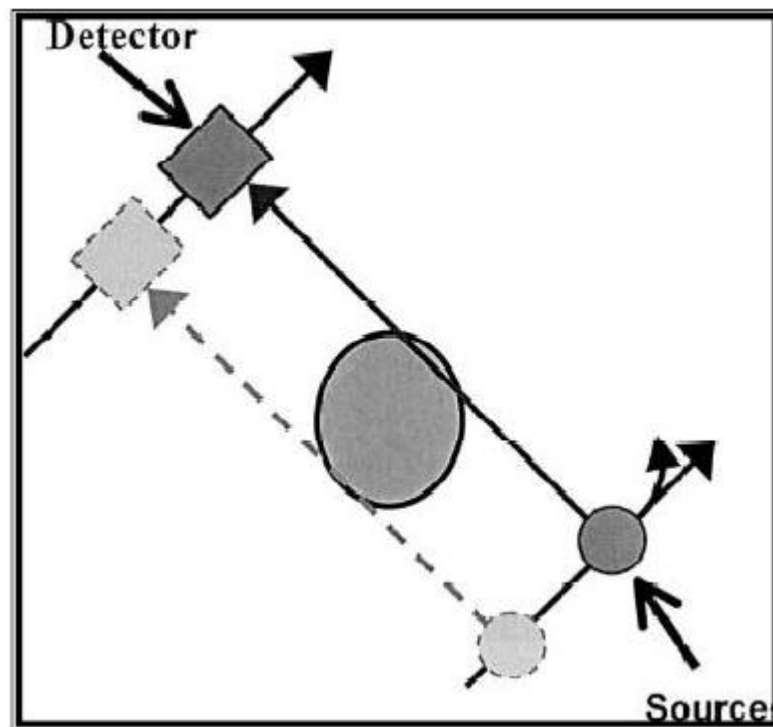
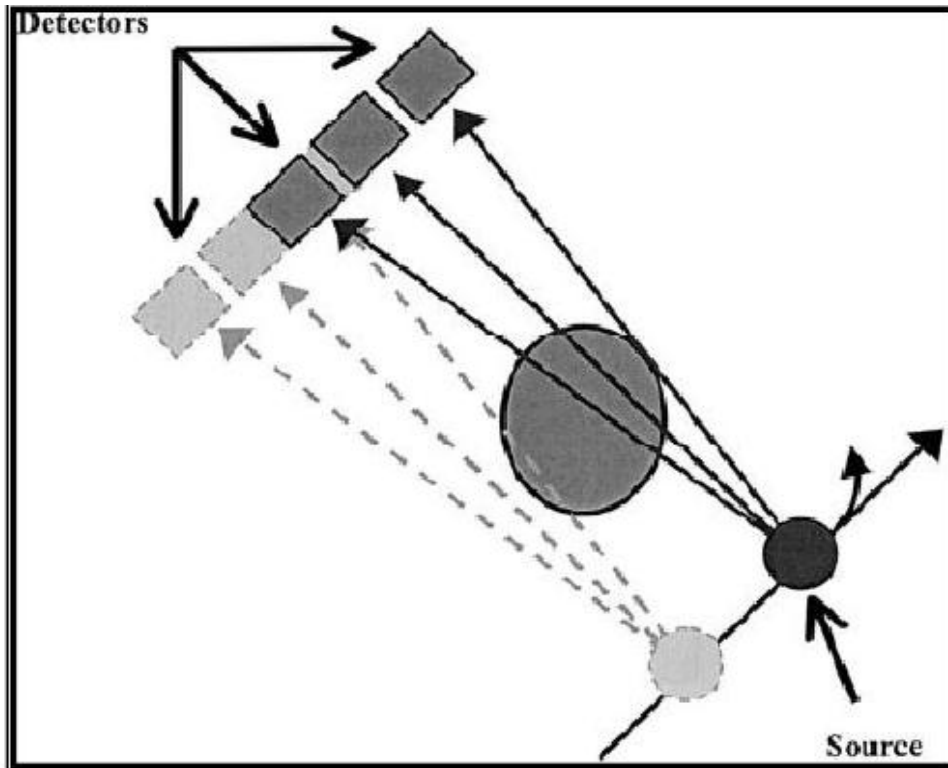


Fig (2.2): Diagram of the first-generation CT scanner, which used a parallel x-ray beam with translate-rotate motion to acquire data. From (Mahesh,2002).

2.2.2 Second-Generation CT Scanners

The main impetus for improvement was in reducing scan time ultimately to the point that regions in the trunk could be imaged. By adding detectors angularly displaced, several projections could be obtained in a single

translation. For example, one early design used three detectors each displaced by 1° . Since each detector viewed the x-ray tube at a different angle, a single translation produced three projections. Hence, the system could rotate 3° to the next projection rather than 1° and had to make only 60 translations instead of 180 to acquire a complete section (Fig 2.3). Scan times were reduced by a factor of three. Designs of this type had up to 53 detectors, were ultimately fast enough (tens of seconds) to permit acquisition during a single breath hold, and thus were the first designs to permit scans of the trunk of the body. Because rotating anode tubes could not withstand the wear and tear of rotate-translate motion, this early design required a relatively low output stationary anode x-ray tube. The power limits of stationary anodes for efficient heat dissipation were improved somewhat with the use of asymmetrical focal spots (smaller in the scan plane than in the z-axis direction), but this resulted in higher radiation doses due to poor beam restriction to the scan plane. Nevertheless, these scanners required slower scan speeds to obtain adequate x-ray flux at the detectors when scanning thicker patients or body parts.



Fig(2.3): Diagram of the second-generation CT scanner, which used translate rotatemotion to acquire data

2.2.3 Third-Generation CT Scanners

Designers realized that if a pure rotational scanning motion could be used, then it would be possible to use higher-power, rotating anode x-ray tubes and thus improve scan speeds in thicker body parts. One of the first designs to do so was the so-called third generation or rotate-rotate geometry. In these scanners, the x-ray tube is collimated to a wide, fan-shaped x-ray beam and directed toward an arc-shaped row of detectors. During scanning, the tube and detector array rotate around the patient (Fig 2.4), and different projections are obtained during rotation by pulsing the x-ray source or by sampling the detectors at a very high rate. The number of detectors varied from 300 in early versions to over 700 in modern scanners. Since the slam-bang translational motion was replaced with smooth rotational motion, higher-output rotating

anode x-ray tubes could be used, greatly reducing scan times. One aspect of this geometry is that rays in a single projection are divergent rather than parallel to each other, as in earlier designs. Beam divergence required some modification of reconstruction algorithms, and sampling considerations required scanning an additional arc of one fan angle beyond 180° , although most scanners rotate 360° for each scan.

Nearly all current helical scanners are based on modifications of rotate-rotate designs. Typical scan times are on the order of a few seconds or less, and recent versions are capable of sub second scan times.

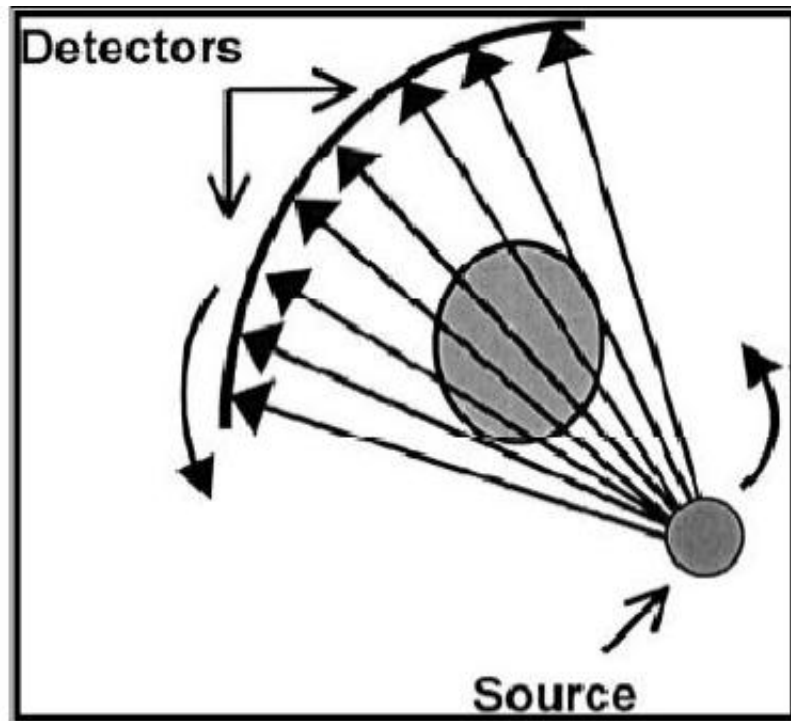


Fig (2.4): Diagram of the third-generation CT scanner, which acquires data by rotating both the x-ray source with wide fan beam geometry and the detectors around the patient. Hence, the geometry is called rotate-rotate motion.

2.2.4: Fourth-Generation CT Scanners:

This design evolved nearly simultaneously with third-generation scanners and also eliminated translate-rotate motion. In this case, only the source rotates within a stationary ring of detectors (Fig 2.5). The x-ray tube is positioned to rotate about the patient within the space between the patient and the detector ring. One clever version, which is no longer produced, moved the x-ray tube out of the detector ring and tilted the ring out of the x-ray beam in a wobbling (nutation) motion as the tube rotated. This design permitted a smaller detector ring with fewer detectors for a similar level of performance. Early fourth generation scanners had some 600 detectors and later versions had up to 4,800. Within the same period, scan times of fourth-generation designs were comparable with those of third-generation scanners. One limitation of fourth generation designs is less efficient use of detectors, since less than one-fourth are used at any point during scanning. These scanners are also more susceptible to scatter artifacts than third-generation types, since they cannot use anti scatter collimators. CT scanners of this design are no longer commercially available except for special-purpose applications. (Mahesh, 2002) Until around 1990, CT technology had evolved to deliver scan plane resolutions of 1–2 lp/mm, but z-axis resolution remained poor and interscan delay was problematic due to the stop-start action necessary for table translation and forcable unwinding, which resulted in longer examination times. The z-axis resolution was limited by the choice of section thickness, which ranged from 1 to 10 mm. For thicker sections, the partial volume averaging between different issues led to partial volume artifacts. These artifacts were reduced to some extent by scanning thinner sections. In addition, even though it was possible to obtain 3D images by stacking thin sections, inaccuracy dominated due to involuntary motion from scan to scan. A

typical 3D reconstruction of this era is shown in Figure 2.7 the step like contours could be minimized by overlapping of CT sections at the expense of a significant increase in radiation to the patient. Also, the conventional method of section-by-section acquisition produced misregistration of lesions between sections due to involuntary motion of anatomy in subsequent breath holds between scans. It was soon realized that if multiple sections could be acquired in a single breath hold, a considerable improvement in the ability to image structures in regions susceptible to physiologic motion could result. However, this required some technological advances, which led to the development of helical CT scanners. (Mahesh, 2002)

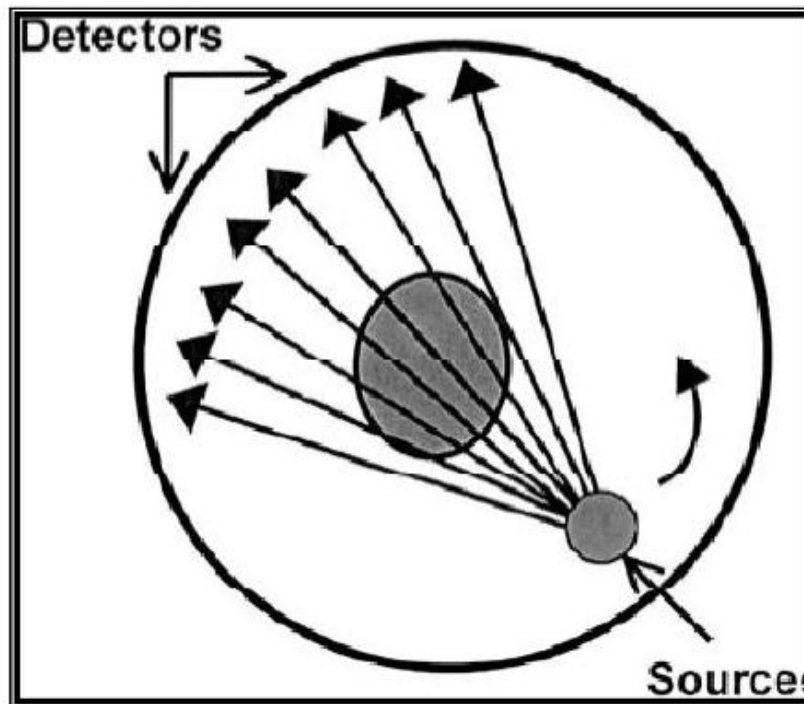


Fig (2.5): Diagram of the fourth-generation CT scanner, which uses a stationary ring of detectors positioned around the patient. Only the x-ray source rotates with wide fan beam geometry, while the detectors are stationary. Hence, the geometry is called rotate-stationary motion. From (Mahesh, 2002)

2.3 Principles of Helical CT Scanners

The development of helical or spiral CT around 1990 was a truly revolutionary advancement in CT scanning that finally allowed true 3D image acquisition within a single breath hold. The technique involves the continuous acquisition of projection data through a 3D volume of tissue by continuous rotation of the x-ray tube and detectors and simultaneous translation of the patient through the gantry opening (Fig 2.6) (Kalender, et al, 1990). Three technological developments were required: slip-ring gantry designs, very high power x-ray tubes, and interpolation algorithms to handle the non-coplanar projection data (Beck, 1996).

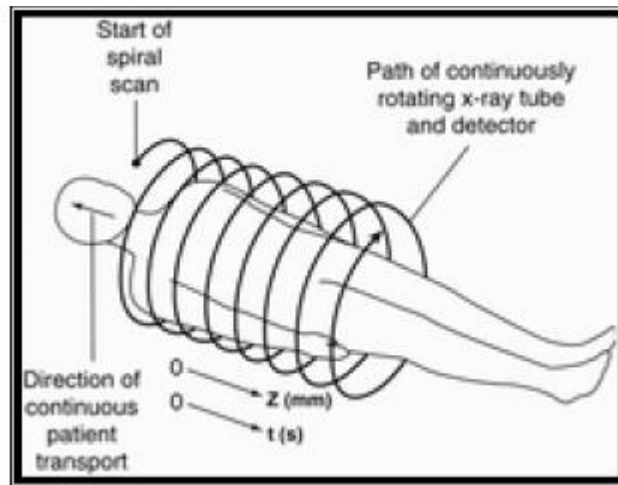


Fig (2.6): Principles of helical CT. As the patient is transported through the gantry, the x-ray tube traces a spiral or helical path around the patient, acquiring data as it rotates. t = time in seconds. (Mahesh, 2002).

2.4 Slip-Ring Technology

Slip rings are electromechanical devices consisting of circular electrical conductive rings and brushes that transmit electrical energy across a moving interface. All power and control signals from the stationary parts of the scanner system are communicated to the rotating frame through the slip

ring. The slip ring design consists of sets of parallel conductive rings concentric to the gantry axis that connect to the tube, detectors, and control circuits by sliding contactors (Fig 2.7).

These sliding contactors allow the scan frame to rotate continuously with no need to stop between rotations to rewind system cables (Brunnett, et al.1994). This engineering advancement resulted initially from a desire to reduce interscan delay and improve throughput. However, reduced interscan delay increased the thermal demands on the x-ray tube; hence, tubes with much higher thermal capacities were required to withstand continuous operation over multiple rotations. (Mahesh, 2002)

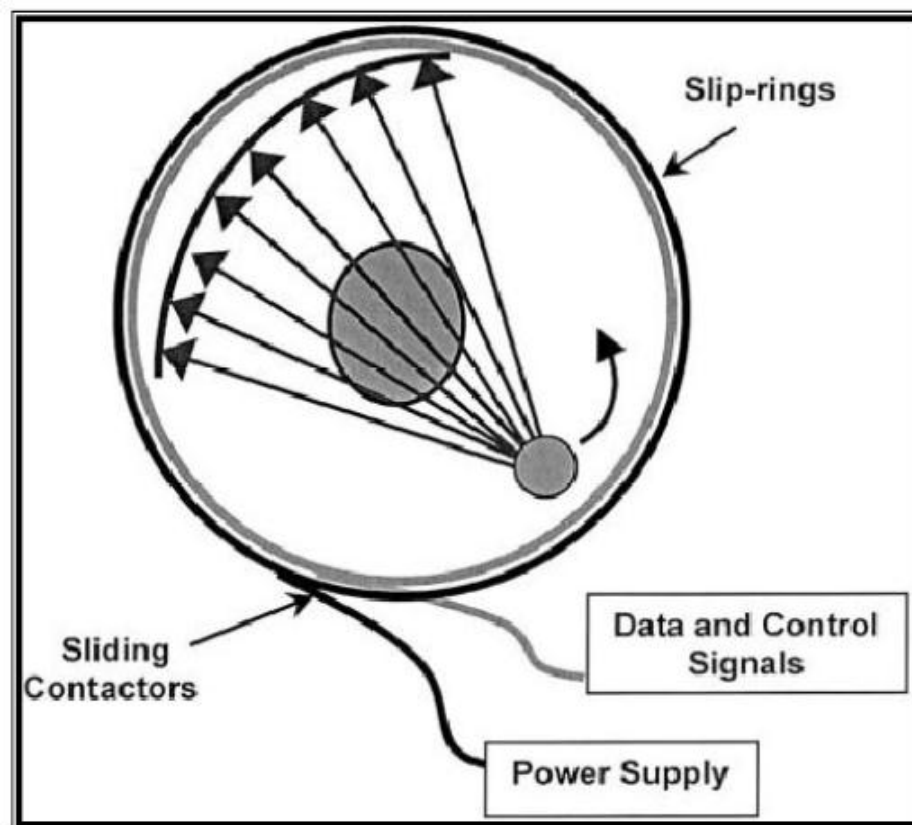


Fig (2.7): Diagram of the slip-ring configuration. Sliding contactors permit continuous rotation of the x-ray tube and detectors while maintaining electrical contact with stationary components.

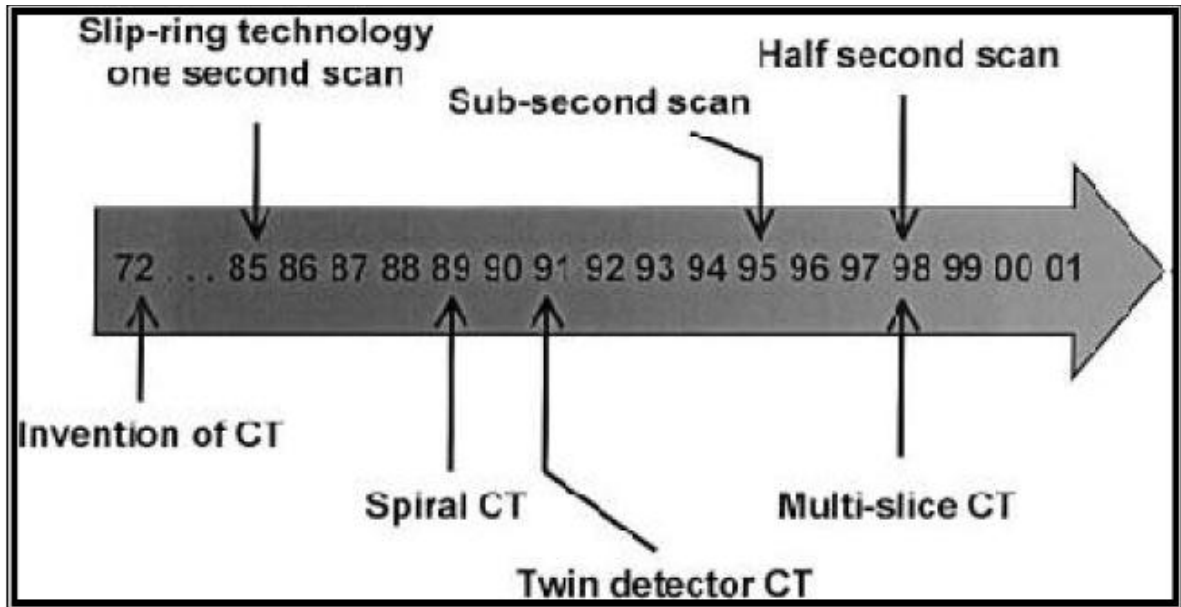


Fig (2.8): Time line of the key technological developments in CT. From (Mahesh,2002).

2.5 Capabilities of Single-Row Detector Helical CT

With the advent of helical CT, considerable progress was made on the road toward 3D radiography. An example of a 3D reconstruction from single-row detector helical scanning is shown in Fig (2.9). Complete organs could be scanned in about 30–40 seconds; artifacts due to patient motion and tissue misregistration due to involuntary motion were virtually eliminated. It became possible to generate sections in any arbitrary plane through the scanned volume. Significant improvements in z-axis resolution were achieved due to improved sampling, since sections could be reconstructed at fine intervals less than the section width along the z axis. Near-isotropic resolution could be obtained with the thinnest ($\square 1$ mm) section widths at a pitch of 1, but this could be done only over relatively short lengths due to tube and breath-hold limitations (Kalender 1995), (Levy, 1995). Higher-power tubes capable of longer continuous operation coupled with faster rotation speeds could scan

greater lengths with higher resolution. The practical limit on such brute force approaches, however, became the length of time a sick patient could reliably suspend breathing. This turns out to be no more than 30 seconds. Even though the z-axis resolution for helical CT images far exceeds that of conventional CT images, the type of interpolation algorithm and the pitch still affect the overall image quality.

The section sensitivity profiles of helical CT images are different compared with those of conventional CT images, which are influenced by the type of interpolation algorithm and the selected pitch.

2.6 Multiple-Row Detector Helical CT

Continued scanner development on the road to a 3D radiograph called for further progress, but single-row detector helical scanners had reached their limits. An obvious improvement would be to make more efficient use of the x-rays that are produced by the tube while improving z-axis spatial resolution; this led to the development of multiple-row detector arrays. The principal difference between single- and multiple-row detector helical scanners is illustrated in Figure (2.9). The basic idea actually dates to the very first EMI Mark I scanner, which had two parallel detectors and acquired two sections simultaneously.

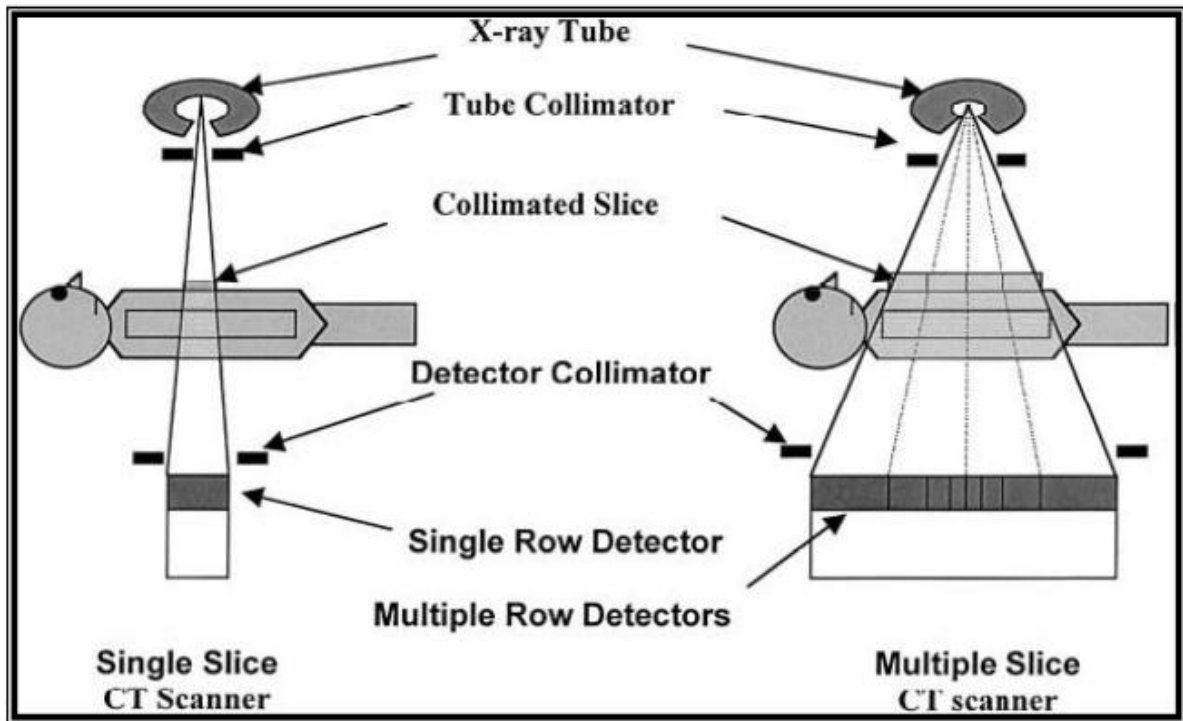


Fig (2.9): Diagram shows the difference between single-row detector and multiple-row detector CT designs.

The multiple-row detector array shown is asymmetrical and represents that of one particular manufacturer. The first helical scanner to use this idea, the CT Twin was launched in 1992. (Mahesh, 2002). This design was so superior to single-row detector designs that all scanner manufacturers went back to the drawing board. By late 1998, all major CT manufacturers launched multiple-row detector CT scanners capable of acquiring at least four sections per rotation. The arrangement of detectors along the z axis and the widths of the available sections vary between the systems. Fig(2.10) illustrates different multiple-row detector array configurations from several manufacturers.

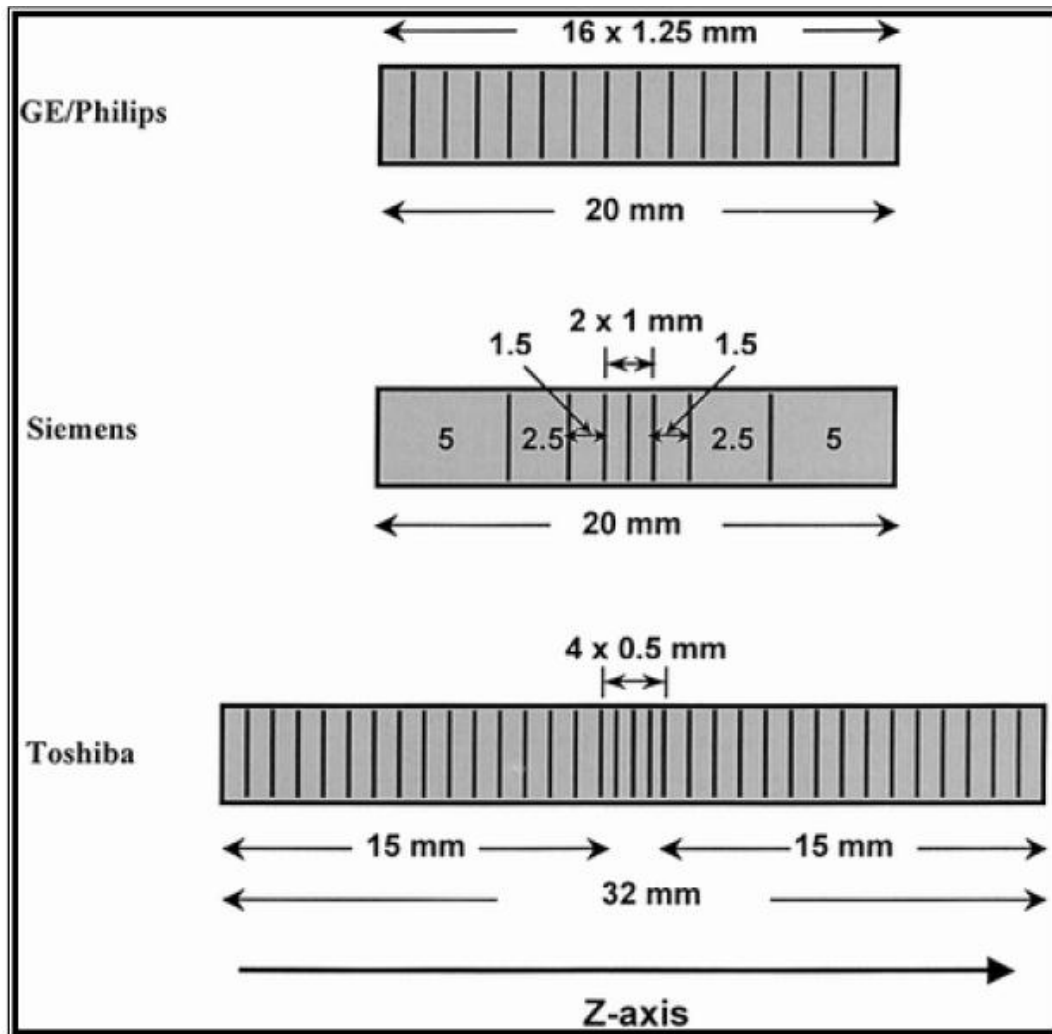


Fig (2-10): Various detector array designs used in multiple-row detector CT Scanners

In single-row detector helical CT designs, scan volume can be increased with an increased pitch at the expense of poorer z-axis resolution, whereas z-axis resolution can be preserved in multiple-row detector designs. For example, if a 10-mm collimation were divided into four 2.5-mm detectors, the same scan length could be obtained in the same time but with a z-axis resolution improved from 10 mm to 2.5 mm. In another example, a multiple-row detector scanner with four 5-mm detectors and a beam width of 20

mm reduces the scan time by a factor of 4–15 seconds for the same z-axis resolution (Mahesh, 2002). By increasing the number of CT scanner detector rows, data acquisition capability dramatically increases while greatly improving the efficiency of x-ray tubes. Further developments in scanner rotational speeds and tube outputs have made isotropic resolution a practical possibility with even better improvements on the horizon. Current multiple row detector scanners can scan large 40-cm volume lengths in less than 30 seconds with near-isotropic resolution and image quality that could not be envisioned at the time of Hounsfield's invention. MDCT systems are CT scanners with a detector array consisting of more than a single row of detectors. The “multi-detector-row” nature of MDCT scanners refers to the use of multiple detector arrays (rows) in the longitudinal direction (that is, along the length of the patient lying on the patient table) MDCT scanners utilize third generation CT geometry in which the arc of detectors and the x-ray tube rotate together. All MDCT scanners use a slip-ring gantry, allowing helical acquisition at rotation

speeds as fast as 0.33 second for a full rotation of 360 degrees of the X-ray tube around the patient. A scanner with two rows of detectors (Mahesh, 2002) had already been on the market since 1992 and MDCT scanners with four detector rows were introduced in 1998 by several manufacturers. The primary advantage of these scanners is the ability to scan more than one slice simultaneously and hence more efficiently use the radiation delivered from the X-ray tube (Fig. 2.11). The time required to scan a certain volume could thus be reduced considerably. The number of slices, or data channels, acquired per axial rotation continues to increase, with 64-detector systems now common (Flohr et al., 2005a ; Flohr et al., 2005b). It is likely that in the coming years even larger arrays of detectors having

longitudinal coverage per rotation > 4 cm will be commercially available. Preliminary results from a 256-detector scanner (12.8 cm longitudinal coverage at the center of rotation) have already been published (Mori et al., 2004). Further, an MDCT system with two x-ray sources is now commercially available, signaling continued evolution of CT technology and applications (Flohr et al., 2006).

MDCT scanners can also be used to cover a specific anatomic volume with thinner slices. This considerably improves the spatial resolution in the longitudinal direction without the drawback of extended scan times. Improved resolution in the longitudinal direction is of great value in multiplanar reformatting (MPR, perpendicular or oblique to the trans axial plane) and in 3-dimensional (3D) representations. Spiral scanning is the most common scan acquisition mode in MDCT, since the total scan time can be reduced most efficiently by continuous data acquisition and overlapping datasets and this allows improved multi-planar reconstruction (MPR) and 3D image quality to be reconstructed without additional radiation dose to the patient.

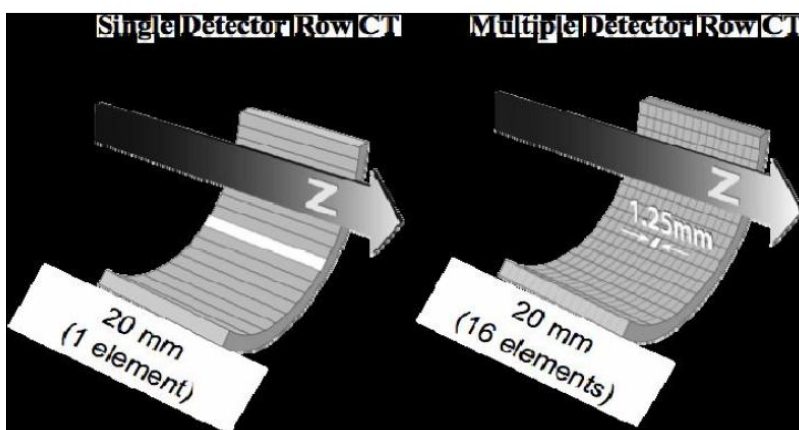


Fig (2.11): single CT detector versus Multi slice CT detector. From (ICRP 32/219,2006).

2.7 CT imaging protocol

The technique used in CT-scanners share most of its characteristics with conventional X-ray imaging, and the prime differences are seen in projection, detection and acquisition as presented in Figure 2.12 below.

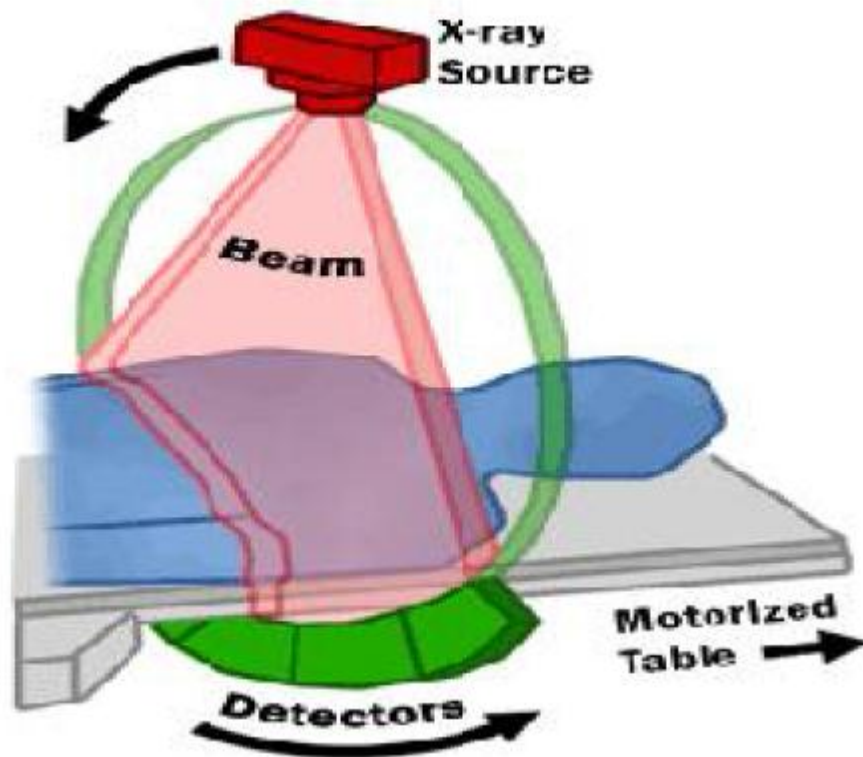


Figure (2.12) Simple overview of a third generation CT-imaging system

2.7.1 Parameters

In order to properly calculate and compare doses, it is imperative to have a standardized nomenclature to ensure that all data is comparative (Kalra, M. Ket al 2006). Without this, it will be difficult to reproduce measurements, and to develop consistent protocols. When performing a CT examination, a number of parameters are defined by the operator. The thesis will cover the

parameters deemed important for correct, uniform dosimetry: tube current, tube voltage, rotation time, total scan length, slice thickness and pitch. Automatic exposure control (AEC) and iterative reconstruction will be briefly covered, as their impact on dose and image quality is more of a qualitative influence than a quantitative one.

2.7.1.1 Tube current

The tube current [mA] influences the number of photons exiting the X-ray tube, as it determines the number of electrons leaving the cathode. The tube current is directly proportional to radiation dose, and as such is a prime parameter in adjusting the dose. Instead of tube current is sometimes used the tube-current time-product [mAs], which is the tube current multiplied with the scan time.

2.7.1.2 Tube Voltage

The tube voltage [kV] determines the voltage across the anode and cathode of the X-ray tube, and therefore the acceleration of the electrodes across the interior vacuum. This determines the kinetic energy of the electrodes when they reach the anode, and therefore the number of interactions they can initiate before being absorbed. As a consequence, an increase in tube voltage will increase the dose, all other factors kept constant; however, the increase is not directly proportional as was the case with current. Voltage determines the energy of the electrons, and therefore the energy distribution of the incident X-rays.

It is rarely adjusted from the customary value of 120 kV. Certain examinations use a different voltage, but seldom outside the range of 80 to 140 kV (Kalra, M. K, et al 2006).

2.7.1.3 Rotation Time

The rotation time of the gantry [s] has decreased greatly over the last few decades, with modern scanners having a rotation time in the area of 0.4 seconds. The main consequence of the decreased rotation time is an increase in the noise and a reduction in absorbed dose. To avoid the noise, it is customary to increase the tube current accordingly (M. K., Maher, et al 2004).

2.7.1.4 Total Scan Length

It is apparent that the total scan length [cm] influence the absorbed dose, as an increase in scan length will expose a larger part of the patient to radiation. Therefore, it is imperative that scan length is to be limited to cover just the diagnostically relevant part of the patient; otherwise, an unnecessary increase in dose will be seen (ICRP, 2000). This is relatively easy with SSCT; however, the situation is more complicated for MSCT. At the initiation of the scan, the X-ray tube will be activated the moment the first row of detectors reach the diagnostic area. The X-ray beam will irradiate the entire detector array, but only the first row of detectors will be acquiring image data. The remaining detector rows will not acquire data, but the area will still be irradiated. This is called over scan, and a small degree of over scan is required for correct reconstruction. As the table moves, more rows of detectors are entering the diagnostic area, contributing to the image. At the reverse end of the patient, the same scenario occurs, and an noteworthy part of the dose is absorbed in the patient outside the diagnostic area

(M. K., Maher et al 2004).

2.7.1.5 Slice Thickness

In SSCT, with only a single row of detectors, the slice thickness [cm] is determined by simple collimation. The maximum slice thickness is limited by the width of the individual detector element (typically 10 mm (M. K.,

Maher,etal 2004)), and by collimating the beam, this thickness can be decreased. In otherwords, the width of the beam is equal to slice thickness. In MSCT, the width of each individual detector element in the longitudinal direction determines the minimum slice thickness, and by merging multiple adjacent detector elements during detection, one can increase the slice thickness.

This has a significant impact on image quality, as thin slices have better spatial resolution compared to thick slices, but lower SNR. To address the decrease in SNR, it is necessary to increase for instance the tube current, resulting in a significant increase in dose to the patient (Kalender, et al, 2005).

2.7.1.6 Pitch

With the prevalence of helical MSCT, it is necessary to incorporate the incremental movement of the table, in relation to the irradiated area. This is defined as pitch, being the increment of the table per rotation, divided by the width of the beam. In Figure 2.13 below, a 4-slice MSCT is rotated twice around the patient, resulting in the acquisition of eight slices in pairs of two (indicated by color). The slices are in reality at an incline, as the patient is moving during exposure.

$$\text{pitch} = \text{table feed per rotation} / \text{collimation}$$

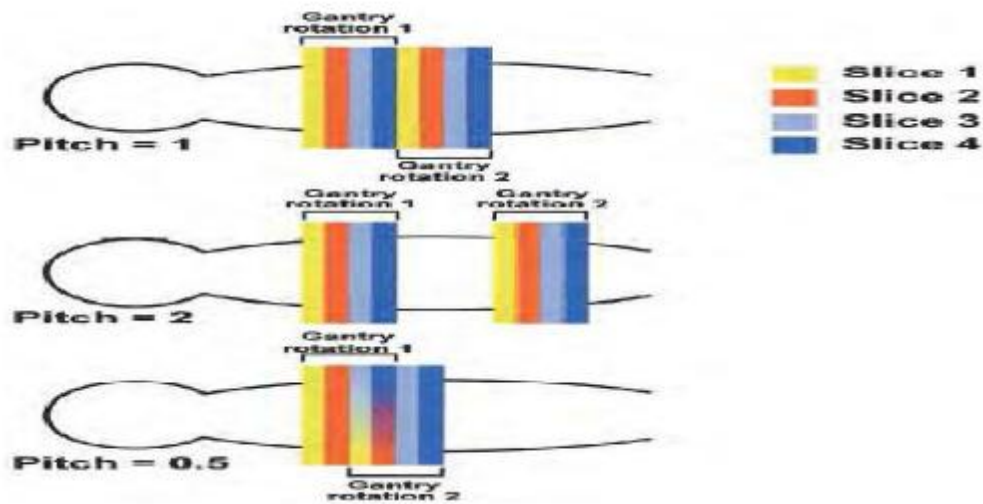


Figure (2.13) The effect of pitch on irradiated area, with a overlap for pitch < 1

2.7.1.7 Automatic Exposure Control

Technological advances lead to the development of a technique where the tube current is modulated in real-time, in order to minimize the dose while retaining image quality. This technique, Automatic Exposure Control(AEC) varies the tube current during exposure. The variance is relative to patient thickness, optimized to achieve dose distribution defined by a desirable image quality. It is possible to achieve a significant reduction in dose based on which type of AEC is used: either the exposure varies within a single slice, i.e. in the image plane of the slice, or it is modulated in the longitudinal direction of the patient. It is also possible to combine these two types of AEC.

2.7.2 Protocols

Brain and abdomen. All of the above parameters are defined in protocols, which are a basic set of parameters that are hereafter modified in order to accommodate the individual patient. Protocols serve as basic guidelines for a specific examination on a specific scanner.

2.8 CT Dose and unit

2.8.1 Radiation dose units

The specific units of measurement for radiation dose commonly referred to as effective dose (mSv). Other radiation dose measurement units include; Rad, Rem, Rontgen and Sievert. Because different tissues and organs have varying in sensitivity to radiation exposure, the actual effective dose to different parts of the body for X-ray procedure varies. The term effective dose is used when referring to the dose averaged over the entire body. The effective dose accounts for the relative sensitivities of different tissues exposed. More importantly, it allows for qualification of risk and comparison to more familiar sources of exposure that range from natural background radiation to radiographic medical procedure. As with other medical procedures, X-rays are safe when used with care. Radiologists and X-ray technologists have been trained to use the minimum amount of radiation that is necessary to obtain the needed results. The decision to have an X-ray examination is a medical one, based on the like lihood of benefit from the examination and the potential risk from radiation (ICRP1990, ICRP 1991).

2.8.2 Effective dose

Effective dose is becoming a very useful radiation quantity for expressing relative risk to humans, both patients and other personnel. It is actually a simple and very logical concept. It takes into account the specific organs and areas of the body that are exposed. The point is that all parts of the body and organs are not equally sensitive to the possible adverse effects of radiation, such as cancer induction and mutations (Perry Sprawls.org, Online).

For the purpose of determining effective dose, the different areas and organs have been assigned tissue weighting factor (WT) values. For a specific organ or body area the effective dose is:

Effective Dose (Gy) = Absorbed Dose (Gy) x WT (2.1)

If more than one area has been exposed, then the total body effective dose is just the sum of the effective doses for each exposed area. It is as simple as that.

Now let's see why effective dose is such a useful quantity. There is often a need to compare the amount of radiation received by patients for different types of X-ray procedures, for example, a chest radiograph and a CT scan. The effective dose is the most appropriate quantity for doing this. Also, by using effective dose it is possible to put the radiation received from diagnostic procedures into perspective with other exposures, especially natural background radiation (PerrySprawls.org, Online).

It is generally assumed that the exposure to natural background radiation is somewhat uniformly distributed over the body. Since the tissue weighting factor for the total body has the value of one (1), the effective dose is equal to the absorbed dose. This is assumed to be 300 mrad in the illustration.

Let's look at an illustration. If the dose to the breast, MGD, is 300 m rad for two views, the effective dose is 45 mrad because the tissue weighting factor for the breast is 0.15.

What this means is that the radiation received from one mammography procedure is less than the typical background exposure for a period of two months.

2.9.1 Computed tomography dose index (CTDI)

The 'Computed Tomography Dose Index (CTDI)' is the fundamental CT dose descriptor. By making use of this quantity, the first two peculiarities of CT scanning are taken into account: The CTDI (unit: Milligray (mGy)) is derived from the dose distribution along a line which is parallel to the axis of rotation for the scanner (=z axis) and which is recorded for a single rotation of X-ray source. (Fig.2.14) illustrates meaning of the term: CTDI is the equivalent

of the dose value inside the irradiated slice (beam) that would result if the absorbed radiation dose profile were entirely concentrated to a rectangular of width equal to the nominal beam width with N being the number of independent (i.e. non-overlapping) slices that are acquired simultaneously. Accordingly, all dose contributions from outside the nominal beam width, i.e. the areas under the tails of the dose profile, are added to the area inside the slice (Nagel 2007).

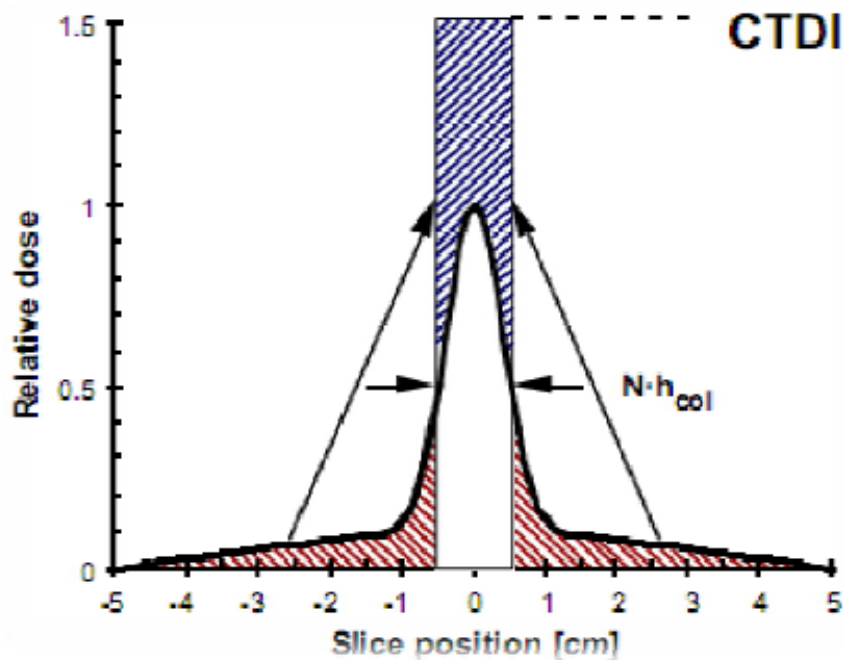
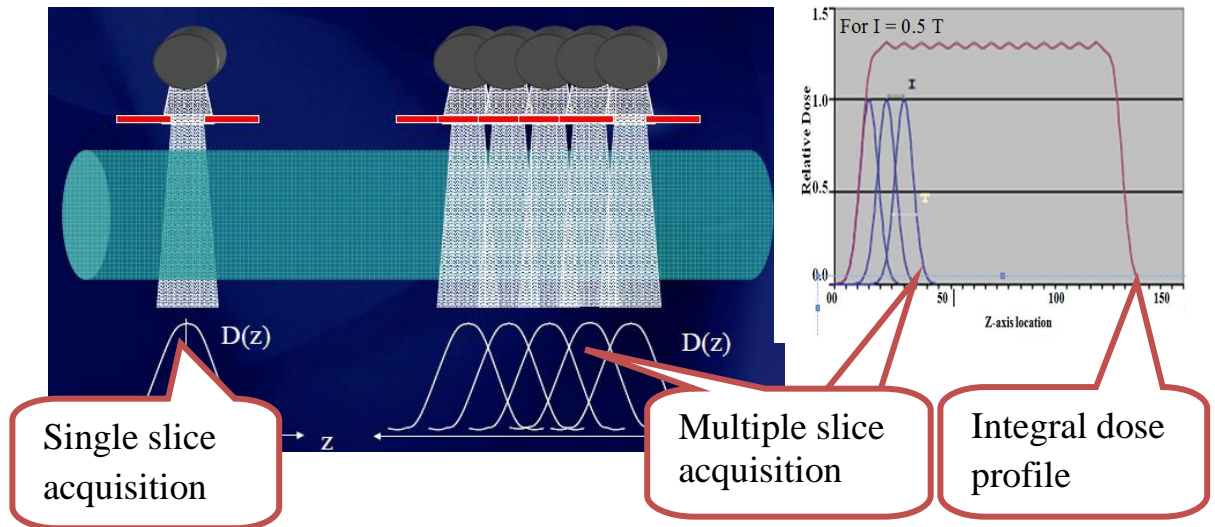


Figure (2.14) Illustrates meaning of the term: CTDI

The local tissue dose from a single slice is not the same as the dose in the very same tissue when additional adjacent slices are made, because each additional slice scatters radiation into adjacent slices.

$D(z)$ = dose profile along z -axis from:

Even if slices are non-overlapping (and ignoring beam penumbra) scatter tails of multiple contiguous scans overlap and contribute to an increased integral dose Profile, which is a Function of:



- an Profile Width (T)
- Number of scans (N)
- Spacing (I) between slices

- Computed Tomography Dose Index (CTDI) – defined:

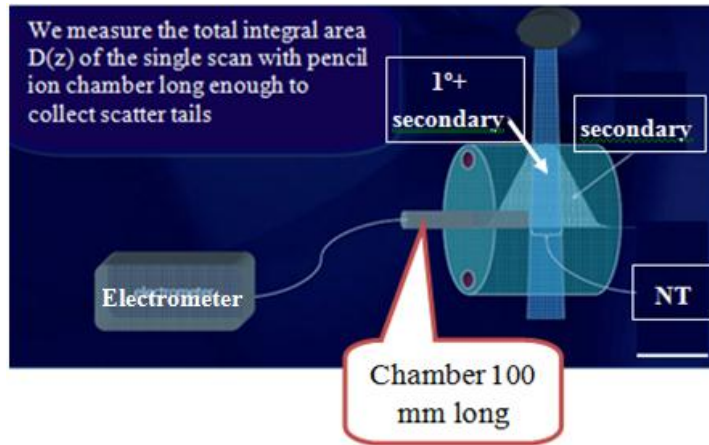
Total area of $D(z)$ under width T of central scan of multiple scan profile = total area of single scan dose profile (including scatter tails).

CTDI is calculated from measured $D(z)$

Calculating CTDI:

- Single axial scan (in phantom to emulate patient scatter) of nominal *beam*

thickness T is given by:



2.10 Image quality

2.10.1 Contrasts

Contrast is a measure of the relative signal difference between two locations in an image, especially between the image of an object and the background (Cunningham IA ,2000). The contrast of an imaging system is described by the characteristic response curve of the system. This curve has a typical Sshape for a screen-film system and an X-ray film can easily become over- or underexposed because there for most systems is not a simple linear relationship. In digital systems the characteristic curve is generally linear and thus the risk of over- or underexposure can be avoided; however, if the user is not properly trained, there is an obvious risk that the patient exposure can be unnecessarily high since a digital detector does not set the limit as film does with respect to film blackening.

2.10.2 Resolution

Image degradation due to spatial resolution properties can be characterized effectively by observing the response of a system to known, simple objects and such information can be used to predict the response to more complex objects. The point spread function (PSF), line spread function (LSF) and edge spread function (ESF) are the response of a system to point, line and step-edge objects, respectively. The modulation transfer function (MTF) of a system is defined as its response to a sinusoidal input; it specifies the relative amplitude of the output signal as a function of the spatial frequency of the sinusoid. In general, the response will decrease as the frequency increases. The MTF curves can be derived simply by computing the two-dimensional Fourier transform of the PSF or, by the one-dimensional transform of the line spread function (Metz CE et al, 1979) A discussion of the measurement of MTF in radiographic systems is given by ICRU Report 54 (1996)

2.10 .3 Noise

The introduction of noise into an imaging process means that the system is no longer deterministic and that its performance must be analyzed using statistical methods.

Random noise is the fluctuations of the signal over an image, as result of a uniform exposure, and can be characterized by the standard deviation of the signal variations over the image of an uniform object. To get a more complete description of the spatial correlation of the noise its Wiener spectrum has to be used which measures the noise power as a function of spatial frequency (Geiger ML, et al 1984). While the difference in signal amplitude of an object relative to the background (contrast) and the noise properties of the image are important characteristics of the image quality, it is the ratio between them

that is most significant indicator of image quality (Dobbins JT .2000). The signal-to noise ratio (SNR) is defined by the following equation:

$$SNR = \Delta S / \sigma \quad (1)$$

Where ΔS is difference in signal of an object and of the background, and σ is standard deviation of the signal distribution in a background area . The SNR of a radiographic system describes the ability of the system to reproduce low-contrast objects. The quantity SNR is especially useful in digital radiography systems, where the image noise can be lowered by increasing the number of photons in the image and thereby also increasing the patient dose , and the contrast can be varied arbitrarily by changing the slope of the characteristic curve of the system. A combination of the primary physical characteristics (contrast, spatial resolution and noise) into a common quantity will be a measure of the overall imaging capability of a radiographic system. Such a quantity can be used to compare the total image quality of two radiographic systems. For instance, a system with high spatial resolution but with very high in here noise can have lower overall image quality than the system with moderate spatial resolution and low noise. The combination of the primary physical characteristic scan be achieved analytically or indirectly. The detective quantum efficiency (DQE) and the image quality

index (IQI) are performed by combining primary physical characteristics into one equation. The contrast detail resolution test combines the primary physical

Characteristic indirectly, by a study of the visibility of small low-contrast objects in the final image. The detective quantum efficiency is a parameter that describes the overall capability of the system to use the information of the incoming photon fluency distribution for the formation of the image. It is defined as the square of the quotient of the signal-to-noise ratio of the signal

out of the imaging system over the signal-to-noise ratio impinging on the imaging system: $DQE = \{SNR_{out} / SNR_{in}\}$ (2)

Determination of the DQE is made by combining the MTF, the Wiener spectrum and the response of the system, but there is at the moment no widely accepted standard method, although it is a valuable quantity for comparing the performance of various imaging systems especially digital systems. Another method for describing the overall performance of an imaging system is the image quality index (IQI) (Desponds L, 1991). The IQI of an image system is the diameter of the smallest high-contrast sphere that is detectable with the system. The IQI is determined by combining the MTF, the Wiener spectrum and the contrast of the imaging system and is mostly used in mammography (Verdun FR et al, 1996). A tool for quick determination of the performance of an imaging system is the use of a contrast-detail phantom (Thijssen MAO, 1989). The phantom consists of a PMMA slab with cylindrical holes of different diameter and depth or for mammography, gold slices of different diameter and thickness included in a PMMA slab. For a given diameter the observer marks the detail that is on the edge of detection as the smallest visible contrast in the image. Due to the subjective nature of human observers, a detection algorithm may be used by a computer program (Jansen JTM et al, 2000)

2.11 Previous studies

Breiki et al. (2008) Evaluated Radiation Dose and Image Quality for Patients Undergoing Computed Tomography (CT) Examinations, to study the CT practice in some CT units in different hospitals in Egypt, in order to investigate the radiation doses imparted to patients during CT examinations and image quality. Method used to CTDI measurements free-in-air and in quality control (QC) phantom using ion chamber, and hence DLP

calculations. Monte Carlo technique utilizing CTDI measurements to calculate organ and effective doses. Direct approach using TLD and Rando phantom to measure organ dose. Computed Tomography Dose Index (CTDI)_w was calculated for each scan from an average of three measurements in the head phantom and another three measurements in the body phantom. DLP values were estimated for each type of examination. Mean values of CTDI_w had a range of 36.0-69.0 mGy for head and 11.0-30.0 mGy for chest, abdomen and pelvis examinations. Organ dose and hence effective dose, calculated using Monte Carlo simulation technique. The effects of selecting tube KV and mAs on both spatial resolution and low contrast detectability were examined for two groups of KV values (90 and 120), the mAs values were degraded from 100 to 300 mAs in 100 mAs interval in first case, and from 50 to 300 mAs, in 50 mAs interval in second case.

Loubele et al. (2008) investigated Image quality vs. radiation dose of four cone beam computed tomography scanners, To evaluate image quality by examining segmentation accuracy and assess radiation dose for cone beam CT (CBCT) scanners. Methods: A skull phantom, scanned by a laser scanner, and a contrast phantom were used to evaluate segmentation accuracy. The contrast phantom consisted of a polymethylmethacrylate (PMMA) cylinder with cylindrical inserts of air, bone and PMMA. The phantoms were scanned on the (1) Accuitomo 3D, (2) Mercuray, (3) NewTom 3G, (4) i-CAT and (5) Sensation 16. The structures were segmented with an optimal threshold. Thicknesses of the bone of the mandible and the diameter of the cylinders in the contrast phantom were measured across lines at corresponding places in the CT image vs. a ground truth. The accuracy was in the 95th percentile of the difference between corresponding measurements. The correlation between accuracy in skull and contrast phantom was calculated. The radiation dose

was assessed by DPI100,c (dose profile integral 100,c) at the central hole of a CT dose index (CTDI) phantom. Results: The results for the DPI100,c were 107 mGy mm for (1), 1569 mGy mm for (2), 446 mGy mm for (3), 249 mGy mm for (4) and 1090 mGy.mm for (5). The segmentations in the contrast phantom were sub millimeter accurate in all scanners. The segmentation accuracy of the mandible was 2.9 mm for (1), 4.2 mm for (2), 3.4 mm for (3), 1.0 mm for (4) and 1.2 mm for (5). The correlation between measurements in the contrast and skull phantom was below 0.37 mm..

Jumaa Yousif Tamboul, (2014), Measured of adult and pediatric Patient doses during head CT scan The objectives of this study were to measure doses from CT examinations of adult and pediatric patients and to compare the doses with international standards as provided in DRLs. Method used A total of 59 patients (pediatric and adults) were examined at the Department of Radiology, Al -Ribat University Hospital-Khartoum. The mean age was 40.80 years for adults while the mean weight was 70.04 kg and the mean age for pediatric was 5.10 years while the mean weight was 20kg. Result : DLP for adults were 1000.25 mGy.cm, 733.33 for pediatrics. The mean effective dose for adults patient was 0.48 mSv in rang (0.49-0.44) mSv, while for pediatric patients was 0.31mSv in rang between (0.49- 0.11) mSv. The DRL was 1120 mGy.cm, a value which is higher than the European Guidelines on Quality Criteria for Computed Tomography. The study has shown a great need for referring criteria, continuous training of staff in radiation dose optimization concepts. Further studies are required in Jörg Hausleiter et al(2006) Estimated Radiation Dose From Cardiac Multi slice Computed Tomography in Daily Practice the aim of the present retrospective study was (1) to estimate the effective dose from cardiac CT angiography in daily practice, (2) to compare the dose estimates from 16- and 64-slice cardiac CT angiography, and (3) to evaluate

the impact of 2 different strategies on dose savings and image quality with both scanner types. Methods : Radiation dose was estimated for 1035 patients undergoing coronary CTA. Scanning algorithm switch and without an ECG-dependent dose modulation and with a reduced tube voltage were investigated on dose estimates and image quality. Result: radiation dose estimates were 6.4_1.9 and 11.0_4.1 mSv for 16- and 64-slice CTA, respectively (P_0.01). The reduction in radiation dose estimates ranged between 37% and 40% and between 53% and 64% with the use of ECG-dependent dose modulation and with the combined use of the dose modulation and a reduced tube voltage, respectively. The reduction in dose estimates was not associated with a reduction in diagnostic image quality as assessed by the signal-to-noise ratio and by the frequency of coronary segments with diagnostic image quality.

Christophe et al (2004) Assessed Patient, Physician, and Radiologist Awareness of Radiation Dose and Possible Risks this study aimed to determine the awareness level concerning radiation dose and possible risks associated with CT scans among patients, emergency department (ED) physicians, and radiologists. Method s : Adult patients seen in the ED of a U.S. academic medical center during a 2-week period with mild to moderate abdominopelvic or flank pain and who underwent CT were surveyed after acquisition of the CT scan. Patients were asked whether or not they were informed about the risks, benefits, and radiation dose of the CT scan and if they believed that the scan increased their lifetime cancer risk. Patients were also asked to estimate the radiation dose for the CT scan compared with that for one chest radiograph. ED physicians who requested CT scans and radiologists who reviewed the CT scans were surveyed with similar questions and an additional question regarding the number of years in practice. The X2 test of independence was used to compare the three respondent groups

regarding perceived increased cancer risk from one abdominopelvic CT scan
RESULTS: Seven percent (five of 76) of patients reported that they were told about risks and benefits of their CT scan, while 22% (10 of 45) of ED physicians reported that they had provided such information. Forty-seven percent (18 of 38) of radiologists believed that there was increased cancer risk, whereas only 9% (four of 45) of ED physicians and 3% (two of 76) of patients believed that there was increased risk ($\chi^2 = 41.45$, $P < .001$). All patients and most ED physicians and radiologists were unable to accurately estimate the dose for one CT scan compared with that for one chest radiograph

Frederiksen et al. (1995) assessed Effective dose and risk from computed tomography of the maxillofacial complex. This study was therefore undertaken to establish \dot{A} from this radiographic technique. (maxillofacial complex in CT.) Methods : Dosimetry was performed using thermoluminescent dosimeters (TLD). For each scan sequence 64 TLDs were placed in 27 selected sites in the upper portion of a tissue-equivalent human phantom to record the equivalent dose in radiosensitive organs/tissues. Results The greatest equivalent dose recorded was that delivered to the salivary glands during scans of the mandible (20.4 mSv) and the least was that received by the bone marrow during scans of the maxilla (0.11 mSv). With the salivary glands assigned a weighting factor of one half the remainder, the effective doses were 0.1 mSv and 0.76 mSv for the maxilla and mandible respectively. From these data, it was calculated that scanning the maxilla corresponded to a probability of stochastic effects of 8×10^{-6} and for the mandible of $56 \div 10^{-6}$. The total probability was therefore 63×10^{-6} .

Cohnen et al. (2006) investigated Radiation Exposure of Patients in Comprehensive Computed Tomography of the Head in Acute Stroke , This

study To assess patient radiation exposure in comprehensive stroke imaging using multidetector row CT (MDCT) combining standard CT of the head, cerebral perfusion (CTP), and CT angiography (CTA) studies. Methods: Examination protocols for CT and CTA of cerebral and cervical vessels, as well as CTP were simulated using a Somatom Sensation Cardiac 64. Effective doses were derived from measurements with the use of lithium-fluoride thermoluminescent dosimeters (LiF-TLD) at several organ sites using an Alderson-Rando phantom .RESULTS: LiF-TLD measurements resulted in effective doses of 1.7 mSv for CT, 1.9 mSv for CTA of intracranial vessels, and 2.8 mSv for CTA of cervical vessels, respectively. Depending on examination parameters, effective doses varied between 1.1 and 5.0 mSv for cerebral CTP. For CTP, local doses in the area of the primary beam ranged between 114 and 444 mGy.

Chapter three

Material and Method

3.1 Material

Three CT machines were used to collect data during this study. These machines were installed in three private radiological departments. All quality control tests.

Performed for the machine prior any data collection, the tests were carried out by experts from Sudan Atomic Energy Commission (SAEC).

Table (3.1) Showed CT machines were used to collect data during this study

Hospital	manufacture	Model	Detected Type
Hospital 1	General electric	Optima	16
Hospital 2	Toshiba	Aquilion	16
Hospital 3	General electric	Optima	64
Hospital4	General electric	Optima	16

3-2 design of the study

The data of this study collected prospectively, it is a descriptive study intends to evaluate the received dose and the quality of the image obtained with the current exposure setting.

3.3. Population of the study

The data of this study collected from adult patient from three types of CT scan, which include head, chest and abdomen in three hospital in Khartoum state during the period from 2017 to 2018.

3-4 Sample size and type

A total of 111 Patients 60 adult were examined for the abdomen 29 of them were female and the others were males and 34 adult were examined for the brain 15 of them were female and the others were males and 17 adult were examined for the chest 8 of them were female and the others were males there aged ranged 25-75 years

3.5 Method of data collection

The data were collected using a sheet for all patients in order to maintain consistency of the information from display. A data collection sheet was designed to evaluate the patient doses and the radiation related factor. The collected data included , sex, and age; tube voltage and tube current–time product settings; pitch; section thickness; and number of sections, In addition, we also recorded all scanning parameters, as well as the CT dose descriptors CT weighted dose index (in millisievert) and dose-length product (in millisievert centimeters). All these factors have a direct influence on radiation dose. The entire hospital was passed successfully the extensive quality control tests performed by Sudan atomic energy commission and met the criteria of this study. The method of dose measurement is as follows:

Effective Dose (E) in CT given by the following

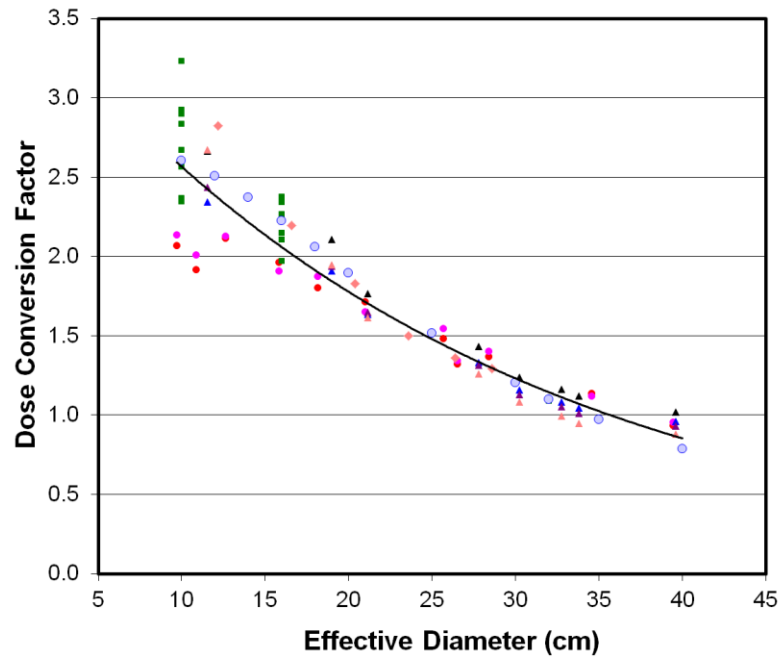
$$E = DLP * k$$

Where k is the tissue weighting factor based on region of body scanned

Representative adult values for k are: Head/Neck = .0031, Head = .0021, Chest = 0.14 and Abdomen = .015

$$SSDE = \text{Dose}_{\text{patient}} \approx \text{CTDI} \times f$$

f is a dose conversion factor that depends on patient size (effective diameter).



Chapter Four Results

Table(4.1) Showed The overall mean of CTDvol, DLP and SSDE values for the three Hospitals

Exam	CTDIvol(mGy)	DLP(mGy)	SSDE(mGy)
Head	60.5	1332.025	61.71
ABD	15.1525	2121.45	16.0025
Chest	13.18	593.09	13.18

Table(4.2) The Mean values of CTDvol, DLP and SSDE values for Hospital 1

Exam	CTDIvol(mGy)	DLP(mGy)	SSDE(mGy)
ABD	13.925	1665.405	14.2035
Chest	13.18	593.09	13.4436

Table(4.3) The Mean values of CTDvol, DLP and SSDE values for Hospital 2

Exam	CTDIvol(mGy)	DLP(mGy)	SSDE(mGy)
Head	60.5	1211.05	61.71
ABD	31.3	1475.05	31.926

Table(4.4) The Mean values of CTDvol, DLP and SSDE values for Hospital 3

Exam	CTDIvol(mGy)	DLP(mGy)	SSDE(mGy)
Head	54.1	8115	55.182
ABD	13.225	5125.5	13.4895
Chest	9.300	2906	7.5888

Table(4.5) Showed Mean effective dose (in mSv) in the three hospitals

Hospitals	Mean	St. Deviation
Hospital1	1.37	12.12
Hospital	5.40	6.34
Hospital	7.66	47.08

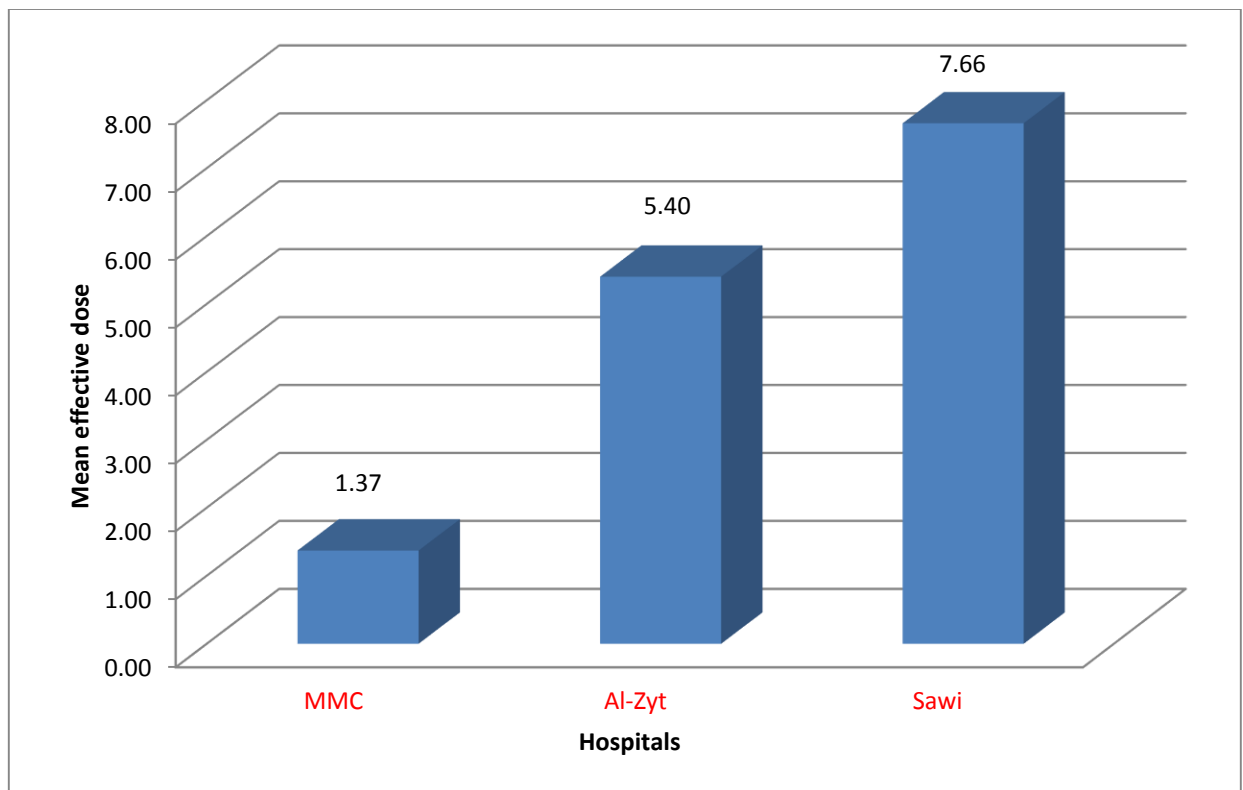


Figure (4.1): Bar graph show the mean effective dose of the three hospitals

Table (4.6): Showed mean SSDE (in mGy) in the three hospitals

Hospital	Mean	St. Deviation
Hospital1	1.88	18.31
Hospital2	4.85	21.40
Hospital3	1.84	54.15

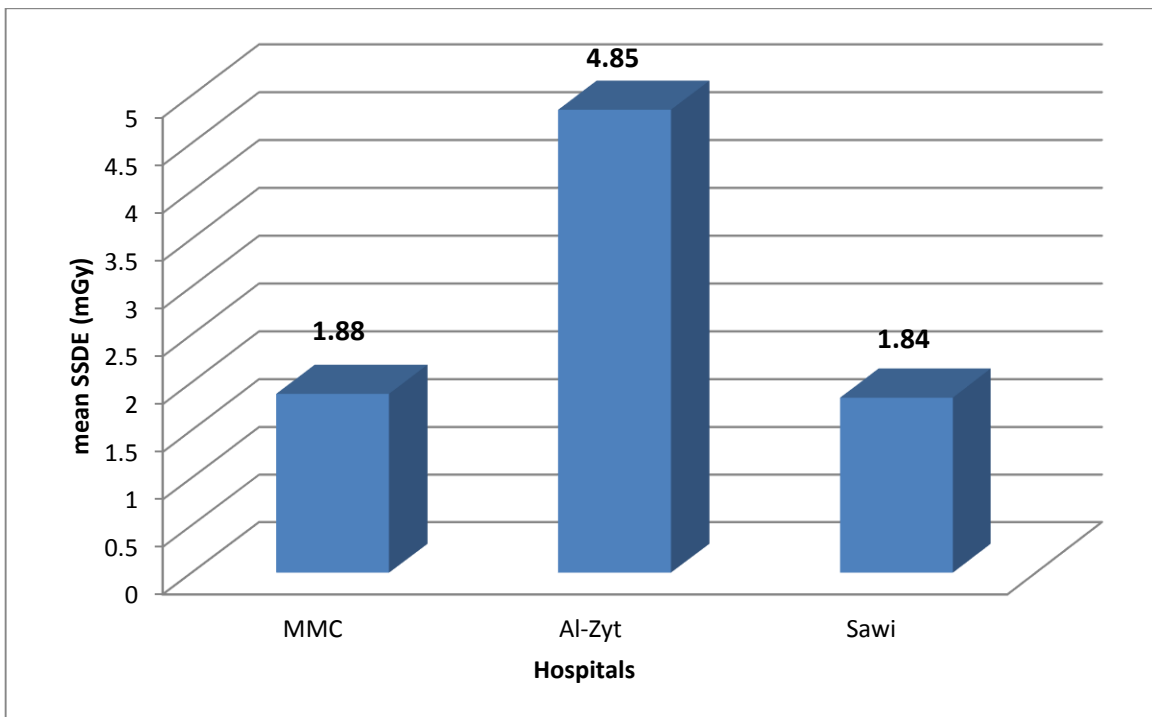


Figure (4.2): Bar graph show mean SSDE in the three hospitals

Table (4.7): Showed Mean effective dose (in mGy) for every exam type

Exam type (our Code)	Mean	St. Deviation
ABD(1)	1.72	14.42
Head(3)	5.65	15.22
Chest(2)	1.08	12.13

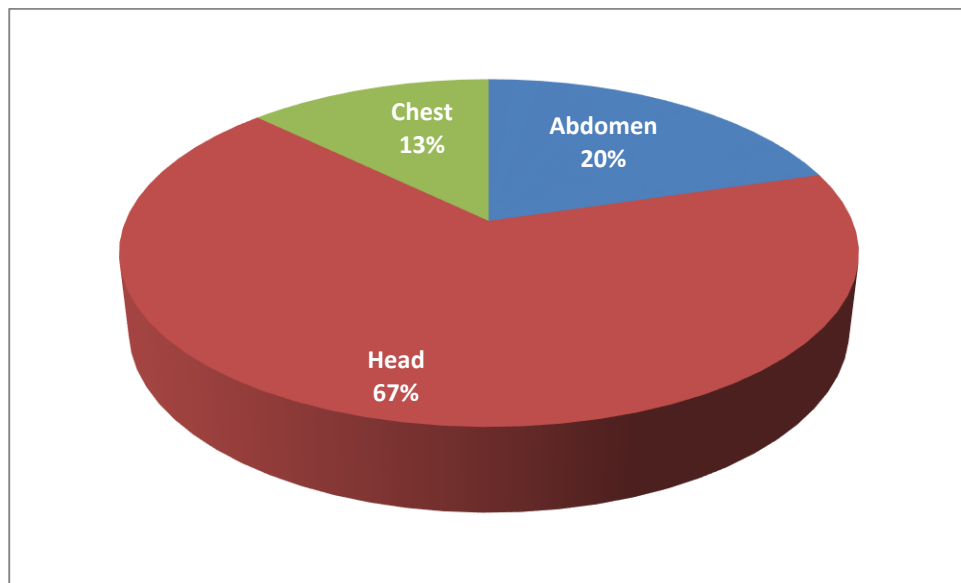


Figure (4.3) Pie graph shows the relative percentage of the mean effective dose (in mGy) for every exam type

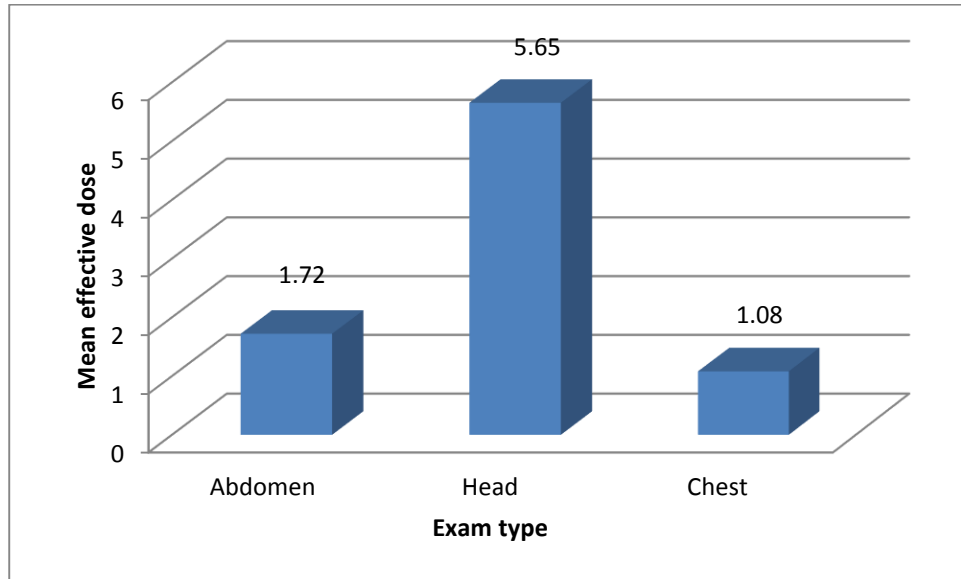


Figure (4.4) Bar graph shows mean effective dose (in mGy) for every exam type

Table (4.8): Showed Mean SSDE (in mGy) in the three hospitals

Exam type	Mean	St. Deviation
ABD	1.29	8.06
Brain	5.65	15.22
Chest	3.29	97.26

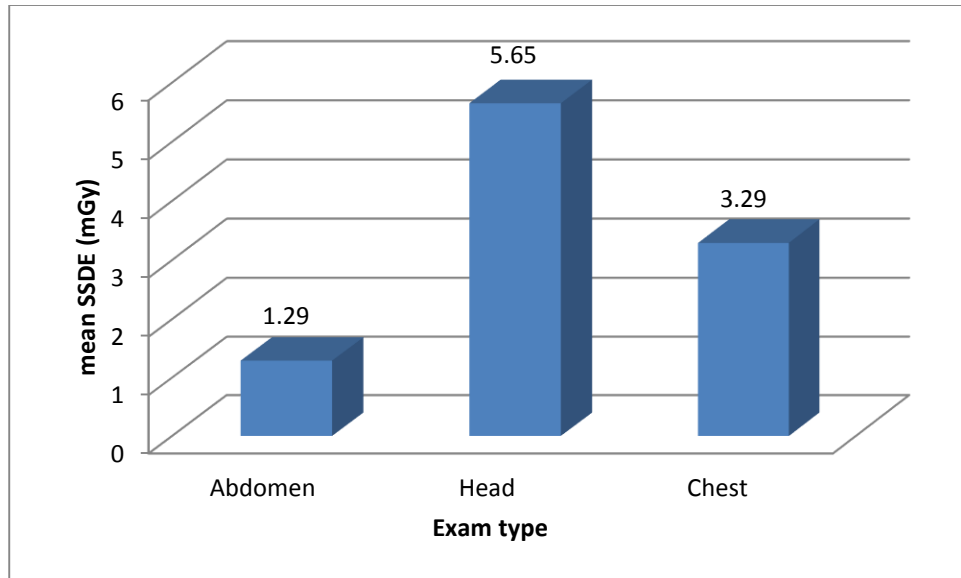


Figure (4.5) Bar graph shows mean SSDE (in mGy) in the three hospitals

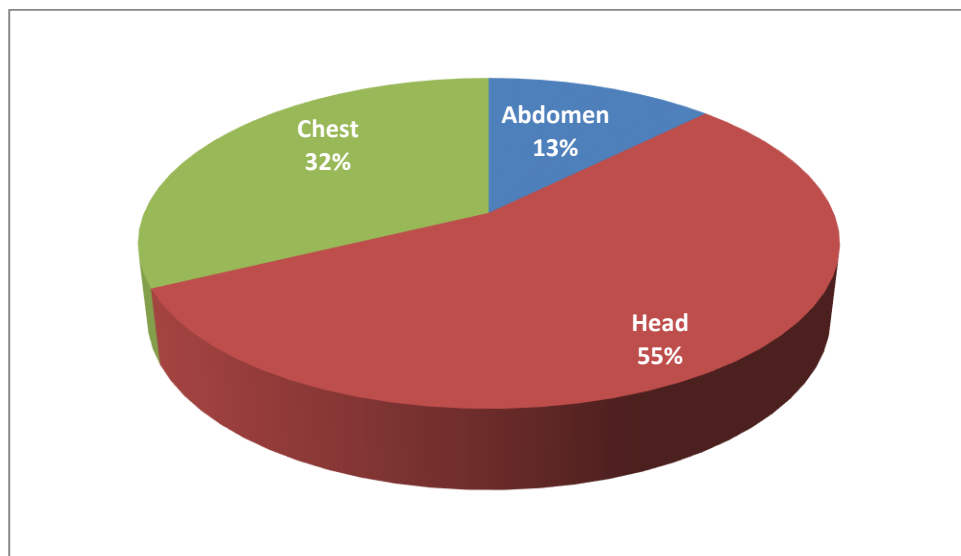
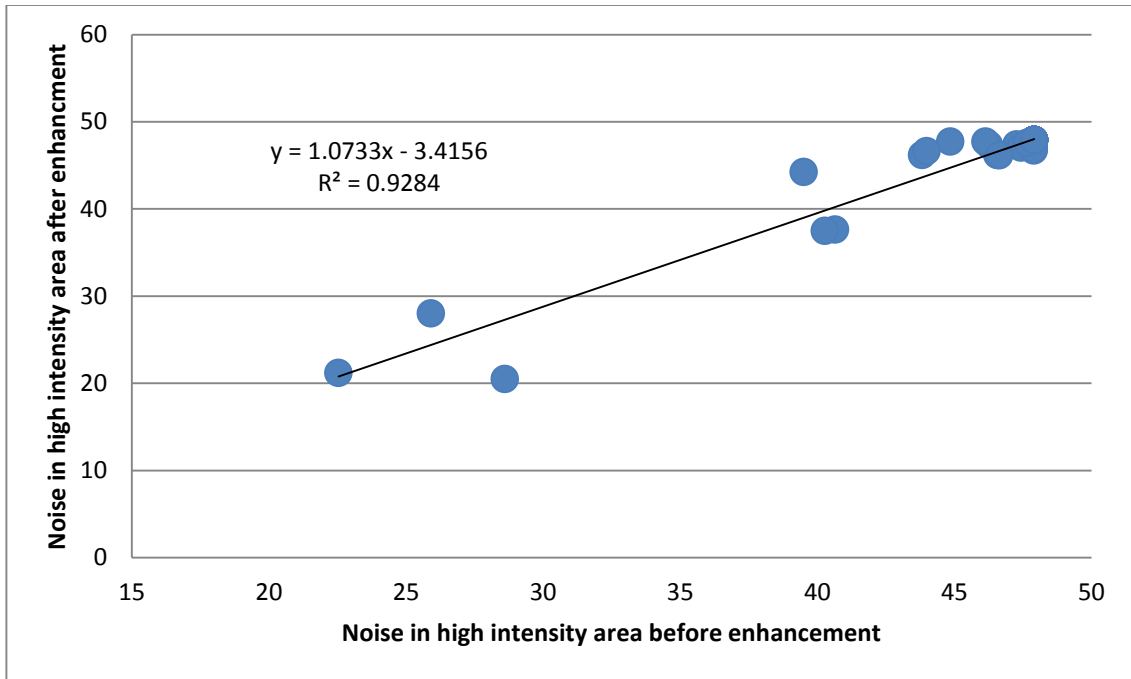
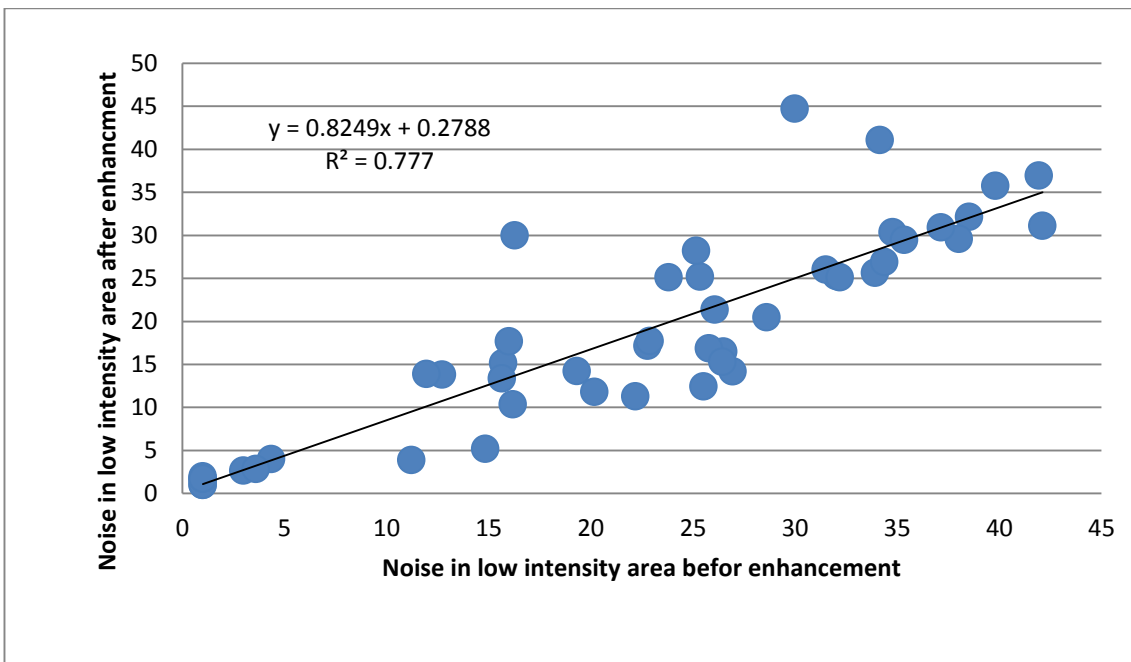


Figure (4.6) Pie graph shows the relative percentage of mean SSDE (in mGy) in the three hospitals

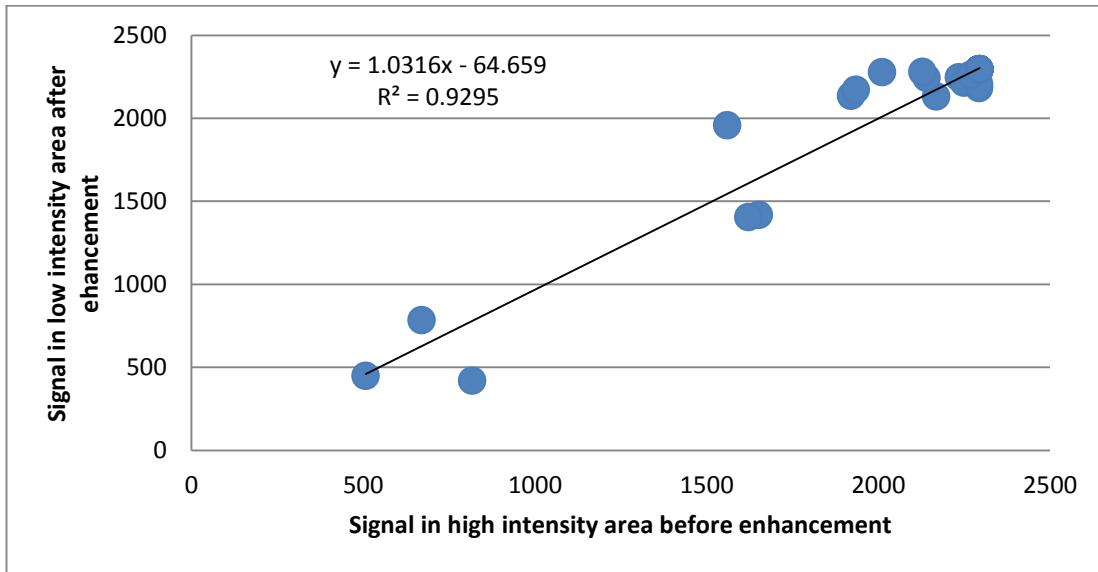


(A)

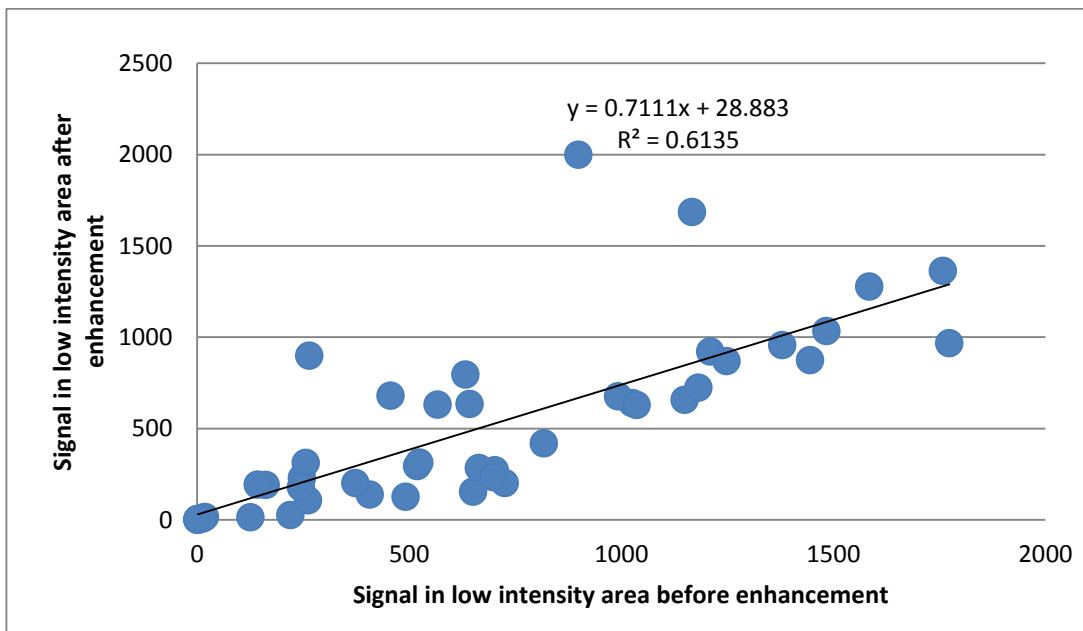


(B)

Figure (4.7): Scatter plot show a direct linear relationship between noise before the enhancement and after enhancement (A) in the high intensity area and (B) low intensity area

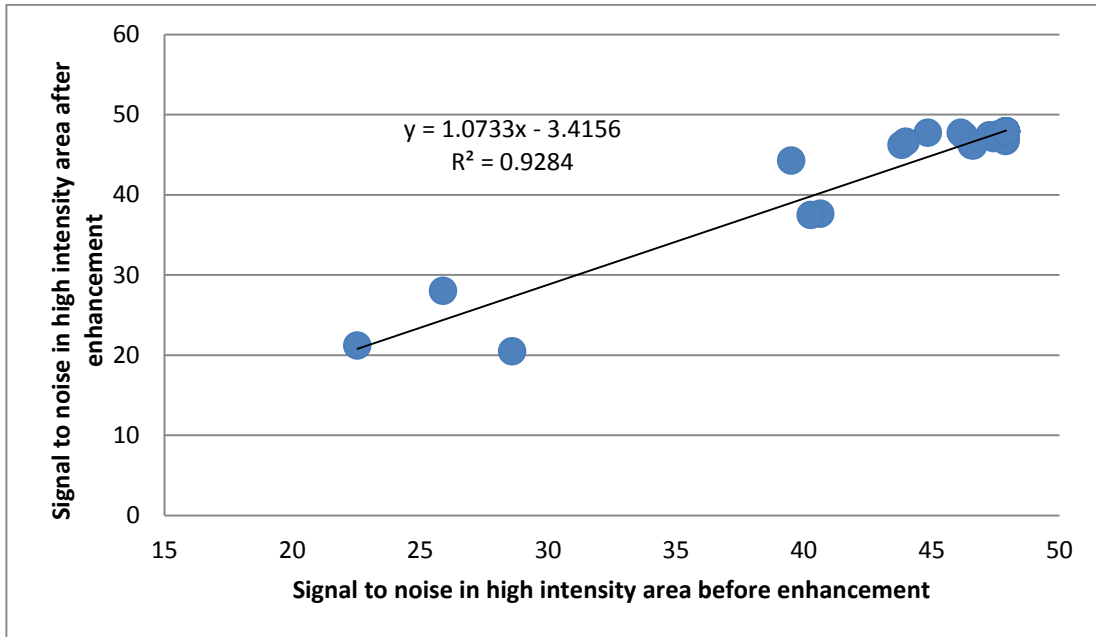


(A)

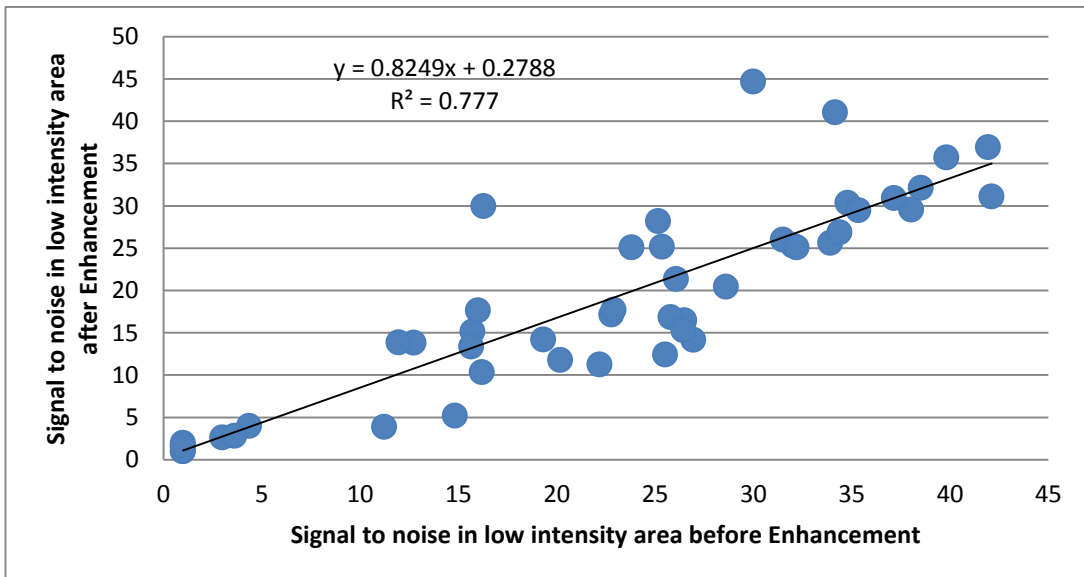


(B)

Figure (4.8): Scatter plot show a direct linear relationship between signal before the enhancement and after enhancement (A) in the high intensity area and (B) low intensity area



(A)



(B)

Figure (4.9): Scatter plot show a direct linear relationship between signal to noise before the enhancement and after enhancement (A) in the high intensity area and (B) low intensity area

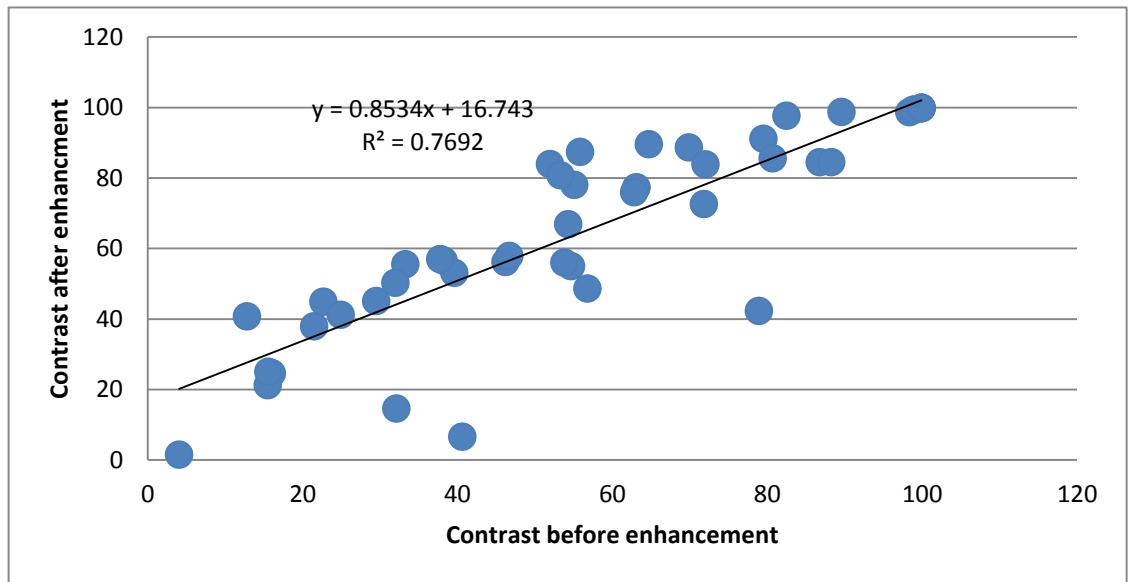


Figure (4.10): Scatter plot show a direct linear relationship between contrast before the enhancement and after enhancement

Table(4-9) Significance paired t-test between the image quality factor before and after enhancement

Before and after enhancement	<i>t</i>	Sig. (2-tailed) (<i>p</i> value)
Signal in high intensity area	-.085	.932
Noise in high intensity area	.276	.784
Signal to noise in high intensity area	.276	.784
Signal in low intensity area	-3.382	0.001
Noise in low intensity area	-11.286	<0.001
Signal to noise in low intensity area	-11.286	<0.001
Contrast	-4.029	<0.001

Table(4.10) The mean, standard deviation, minim and maximum values for the image quality factors

Image quality factors		mean	STD	MIN	MAX
Before enhancement	signal high intensity area	2118.46	416.41	508	2295
	noise high intensity area	45.69	5.58	22.54	47.91
	signal to noise high intensity area	45.69	5.58	22.54	47.91
	signal low intensity area	638.09	518.93	1	1774
	noise in low intensity area	22.01	12.44	1	42.12
	signal to noise low intensity area	22.01	12.44	1	42.12
	Contrast	59	29	4	100%
After enhancement	signal high intensity area	2119.91	445.45	419	2295
	noise high intensity area	45.62	6.21	20.47	47.91
	signal to noise high intensity area	45.62	6.21	20.47	47.91
	signal low intensity area	480.53	471.99	1	1999
	noise in low intensity area	18.42	11.64	1	44.71
	signal to noise low intensity area	17.44	10.85	1	41.06
	contrast	67	28	1%	100%

Chapter Five

Discussion, Conclusion and Recommendation

5-1 Discussion

The results obtained by this study which demonstrates the effective dose in hospital (1, 2 and 3) was $1.37 \pm 12.12 \text{mSv}$, $5.40 \pm 6.34 \text{mSv}$ and $7.66 \pm 47.08 \text{mSv}$ respectively, also the Size specific dose estimate (SSDE) was $1.88 \pm 18.31 \text{mGy}$, $4.85 \pm 21.40 \text{mGy}$ and $1.84 \pm 54.15 \text{mGy}$. As well as CTDvol, DLP and SSDE values in every exam Type firstly head was 60.5mGy , 1332.025mGy and 61.71mGy respectively and for abdomen was 15.1525mGy , 2121.45mGy and 16.0025mGy respectively, finally Chest was 13.18mGy , 593.09mGy and 13.18mGy .

CTDvol of every Exam Type in Three hospitals shown in Figs(4.2,4.3 and 4.4) agree with National DRLs Of CT Examination(Uk) as shown below and agree with Ali (2011).

The DLP for the three hospitals as shown in Figs (4.2,4.3 and 4.4) which concern the chest Exam in hospital 1 agree with National DRLs Of CT Examination (Uk) and other Exams(head and abdomen) were not agree with National DRLs of CT Examination (Uk) because the obtained values were significantly greater than the international one but it agree with Ali (2011) since his study done in the same environment.

For the Effective Dose values in every Exam Type in the three hospitals ABDHead and Chest was 1.72mSv , 5.65mSv and 1.08mSv respectively, this results agree with Ali (2011), Nour (2016) and European Commission (1999)

For image quality which quantified using noise, signal, signal to noise ratio (in low and high intensity) and contrast before and after enhancement; the results show Mean \pm SD, for signal high intensity before 2118.46 ± 416.41 , for

noise is 45.69 ± 5.58 , and for signal to noise 45.69 ± 5.58 . Mean \pm SD, for signal inlow intensity area before 638.09 ± 518.93 , for noise is 22.01 ± 12.44 , and for signal to noise is 22.01 ± 12.44 . Mean \pm SD, for contrast before 59 ± 29 . And Mean \pm SD, for signal high intensity after 2119.91 ± 445.45 , for noise is 45.62 ± 5.58 , and for signal to noise is 45.62 ± 5.58 . Mean \pm SD, for signal inlow intensity area after 480.53 ± 471.99 , for noise is 18.42 ± 11.64 , and for signal to noise is 17.44 ± 10.85 . Mean \pm SD, for contrast after 67 ± 28 .

There is a direct linear relation between the signal in high intensity area before enhancement and after enhancement where the signal after enhancement increase by 1.07 versus one unit of signal before the enhancement as well the graph shown in fig.(4.8) revel strong correlation between the signal before and after, which mean there is a homogenous increase in the signal.

There is a direct linear relation between the signal in low intensity area before enhancement and after enhancement where the signal after enhancement increase by 0.711 versus one unit of signal before the enhancement as well the graph shown in fig.(4.8) revel strong correlation between the signal before and after, which mean there is a homogenous increase in the signal.

There is a direct linear relation between the noise in high intensity area before enhancement and after enhancement where the noise after enhancement increase by 1.031 versus one unit of noise before the enhancement as well the graph shown in fig.(4.7) revel strong correlation between the noise before and after, which mean there is a homogenous increase in the noise.

There is a direct linear relation between the noise in low intensity area before enhancement and after enhancement where the noise after enhancement increase by 0.824 versus one unit of noise before the enhancement as well the graph shown in fig.(4.7) revel strong correlation between the noise before and after, which mean there is a homogenous increase in the noise.

There is a direct linear relation between the signal to noise in high intensity area before enhancement and after enhancement where the signal after enhancement increase by 0.928 versus one unit of signal before the enhancement as shown in fig.(4.9) which reveal strong correlation between the signal before and after, which mean there is a homogenous increase in the signal to noise ratio.

There is a direct linear relation between the signal to noise in low intensity area before enhancement and after enhancement where the signal to noise after enhancement increase by 0.777 versus one unit of signal before the enhancement as well the graph shown in fig.(4.9) reveal strong correlation between the signal to noise before and after, which mean there is a homogenous increase in the signal to noise ratio.

There is a direct linear relation between the contrast before enhancement and after enhancement where the contrast after enhancement increase by 0.853 versus one unit of contrast before the enhancement as well the graph shown in fig.(4.10) reveal strong correlation between the contrast before and after, which mean there is a homogenous increase in the contrast.

5-2 Conclusion

Computed tomography (CT) is an imaging technique which produces a digital topographic image from diagnostic x-ray. It always considered a “high dose” technique, there is growing realization that image quality in CT often exceeds the level needed for confident diagnosis and that patient doses are higher than necessary.

In this study, a total of 111 adult patients underwent the abdominal, head and chest CT scanning exams in Three hospitals were evaluated using effective Dose AND SSDE. The result of this study revealed that the mean effective dose in hospital (1,2 and 3).The Effective dose is higher in hospital3 Than other hospitals and SSDE dose is higher in hospital2 Than other hospitals. And evaluated effective dose in every Exam type is higher brain than other exams. In respect to received dose the CT abdominal examination dose was within the international diagnostic reference level values.

In conclusion the image quality which include noise, signal, signal to noise and contrast in low and high intensity areas can be tested for the applicability and suitability of enhancement before starting the process using the following linear regression equation to estimate the validity as follows:

$$\text{Signal after enhancement (HIA)} = (1.31 \times \text{Signal}) - 64.5$$

$$\text{Signal after enhancement (LIA)} = (0.711 \times \text{Signal}) + 28.8$$

$$\text{Noise after enhancement (HIA)} = (1.07 \times \text{noise}) - 3.41$$

$$\text{Noise after enhancement (LIA)} = (0.824 \times \text{noise}) + 0.278$$

$$\text{SNR after enhancement (HIA)} = (1.07 \times \text{SNR}) - 3.4$$

$$\text{SNR after enhancement (LIA)} = (0.824 \times \text{SNR}) + 0.278$$

$$\text{Contrast after enhancement} = (0.853 \times \text{contrast}) + 16.7$$

Where HIA: High Intensity Area, LIA: Low Intensity Area and SNR: Signal To Noise Ratio

5-3 Recommendation

- CT scan examination for any patient must be justified
- QC program are essential to evaluate the patients dose and machine accurate performance.
- Future studies can be done in order to optimize the radiation dose to establish national diagnostic reference level in Sudan.
- Application of QC program as a routine task in all x-ray department in order to detect possible future problem

References

- AAPM/RSNA Physics Tutorial for Residents 2002.: Topics in CT. McNitt-Gray,
- Ana Teresa Casimiro Nunes, Faculdade de Ciências 2011
Tecnologia Universidade de Coimbra, M.Sc. Thesis.
- Anne Paterson, Donad P. Frush, and Lane Donnelly, 2001 Helical CT of the body: Are settings adjusted for pediatric patient? AJR Vol.176. pp. 297-301.
- Brenner DJ, Hall EJ. Computed tomography: an increasing source of radiation exposure. N Engl J Med 2007; 357: 2277-2284.
- Cattin, P. Principles of Medical Imaging. [Presentation] Basel : University of Basel, 2010.
- Christoph I. Lee, AB Andrew H. Haims, MD Edward P. Monico, MD James A. Brink, MD Howard P. Forman, MD, MBA (2004). *Diagnostic CT Scans: Assessment of Patient, Physician, and Radiologist Awareness of Radiation Dose and Possible Risks*. 398 _ Radiology .
computed tomography of the maxillofacial complex. 58
Dentomaxillofac. Radiol., Vol. 24
- coronary CT angiography performed with a 320-detector row volume scanner. Radiology. 2010;254:698–706.
- Cunningham IA (2000) Applied linear systems theory. In Beutel J, Kundel HL, Van Metter RL (eds) Handbook of medical imaging. SPIE Press, Bellingham, pp 79–159.
- Delapaz RL, Nikoloff E, Dutta A, Brenner DJ: Radiation dose from single heartbeat
- Dobbins JT (2000) Image quality metrics for digital systems. In Beutel J, Kundel HL, Van Metter RL (eds) Handbook of medical imaging. SPIE Press,

Bellingham, pp 161–222 Desponds L, Depeursinge C, Grecescu M, Hessler C, Samiri A, Valley JF (1991) Image quality index (IQI) for screen-film mammography. *Phys Med Biol* 36:19–33.

Einstein AJ, Elliston CD, Arai AE, Chen MY, Mather R, Pearson GD, European Commission. European guidelines on quality criteria for computed tomography EUR 16262 En, Luxemburg (1999).

Flohr TG, Schaller S, Stierstorfer K, Bruder H, Ohnesorge BM, Schoepf UJ. Multi-detector row CT systems and image-reconstruction techniques.

G Breiki, Y Abbas, M EL-Ashry , H Diyab, (2008). **Evaluation of Radiation Dose and Image Quality for Patients Undergoing Computed Tomography (CT) Examinations.** *IX Radiation Physics & Protection Conference, 15-19 November 2008, Nasr City - Cairo, Egypt.*

Giger ML, Doi K, Metz CE (1984) Investigation of basic imaging properties in digital radiography, vol 2. Noise Wiener spectrum. *Med Phys* 11:797–805

Goldman LW. Principles of CT: radiation dose and image quality. *J Nucl Med Technol.* 2007;35:213–225.

Goldman LW. Principles of CT and CT technology. *J Nucl Med Technol.* 2007;35:115–128. Abstract/FREE Full Text.

Gosling O, Loader R, Venables P, Rowles N, Morgan-Hughes G, Roobottom C, Cardiac CT: are we underestimating the dose? A radiation dose study utilizing the 2007 ICRP tissue weighting factors and a cardiac specific scan volume. *Clin Radiol.* 2010;65:1013–7.

Hounsfield GN. Picture quality of computed tomography. *AJR.* 1976;127:3–9. MedlineGoogle Scholar

http://www.icrp.org/Health_risks.pdf. Accessed on 12.04.07.

<http://www.impactscan.org/reports/Report06012.htm>. Accessed March 26, 2008.

https://en.wikipedia.org/wiki/CT_scan 28/5/2017

ICRP. Managing Patient Dose in Computed Tomography. s.l. : ICRP Publication 87, 2000.

International Commission of Radiological Protection. Recommendation of the International Commission of Radiological Protection. Biological and Epidemiological Information on Health Risk Attributable to Ionizing Radiation. International Commission on Radiation Units and Measurements, ICRU (1996) Medical Imaging: the assessment of image quality, ICRU Report 54. ICRU Bethesda, Maryland

Jansen JTM, Zoetelief (2000) Computer aided assessment of image quality for mammography using a contrast detail phantom. *Rad Prot Prot Dos* 90:181–184

Jerrold T. Bushberg, J. Antony Seibert, Edwin M. Leidholdt, JR. John M. Boone 2002, *The Essential Physics for Medical Imaging*, second edition, Jörg Hausleiter, MD; Tanja Meyer, MD; Martin Hadamitzky, MD; Ester Huber; Maria Zankl, MSc; Stefan Martinoff, MD; Adnan Kastrati, MD; Albert Schömig, MD (2006). **Radiation Dose Estimates From Cardiac Multislice Computed Tomography in Daily Practice.**

Circulation.; 113:1305-1310.

Judy PF. CT image quality and parameters affecting the CT image. In: Goldman LW, Fowlkes JB, eds. 2000 Syllabus: Categorical Course in Diagnostic Radiology Physics—CT and US Cross-Sectional Imaging. Oak Brook, IL: Radiological Society of North America; 2000:117–125. Google Scholar.

Julian Simpson, Computed Tomography, General Practitioner Volume
6Number 3 1999 505.

Jumaa Yousif Tamboul, Mohamed Yousef,,Sawsan Suliman, Abdelmoneim
Sulieman (2014).**Measurement of adult and pediatric Patient doses during
head CT scan.** Journal of American Science;10(2).

Kalender WA, Wolf Heiko, SuessChristoph et al. Dose reduction in CT by
online

Kalender, W.A. Computed tomography: fundamentals, system technology,
image quality, applications. Chichester : Wiley, 2005.

Kalra, M. K. and Saini, S. 241:657-660, s.l. : RSNA, December
2006,Radiology.

Keith J. Strauss Marilyn J. Goske Image Gently: Ten Steps You Can Take
toOptimize Image Quality and Lower CT Dose for Pediatric Patient, AJR
2010;194:868-873.

Lewis M, Keat N, Edyvean S. 16 Slice CT scanner comparison report
version14. Report 06012, Feb-06. Available at:

M Loubele, R Jacobs, F Maes, K Denis, S White, W Coudyzer, I Lambrichts,
D van Steenberghe, and P Suetens(2008). **Image quality vs radiation dose of
four cone beam computed tomography scanners.** Dentomaxillofacial
Radiology37, 309–318

M. CohnenH.-J. WittsackS. AssadiK. MuskallaA. RingelsteinL.W. PollA.
SalehU. Mo` dder (2006). **Radiation Exposure of Patients in
ComprehensiveComputed Tomography of the Head inAcute Stroke.**

AJNR Am J Neuroradiol 27:1741– 45

M.F. 22:1541-1553, s.l. :RadioGraphics,

Mahadevappa Mahesh, John C. Scatarige, Joseph Cooper and Elliot

K.Fishman, AJR:177, December (2001).

Martin CJ: Effective dose: how should it be applied to medical exposures?
BrJRadiol. 2007;80:63947.

McCollough CH, Zink FE. Performance evaluation of CT systems. In:
Goldman LW, Fowlkes JB, eds. 2000 Syllabus: Categorical Course in
Diagnostic Radiology Physics—CT and US Cross-Sectional Imaging. Oak
Brook, IL: Radiological Society of North America; 2000:189–207. Google
Scholar

Mettler, F.A., et al. “Effective doses in radiology and diagnostic nuclear
medicine: a catalog.” Radiology, July 2008: 248(1):254–263.

Metz CE, Doi K (1979) Transfer function analysis of radiographic
imaging systems. Phys Med Biol 24:1079–1106

N.L. Frederiksen, B.W. Benson and T.W. Sokolowski (1995). **Effective dose
and risk assessment from**

Philips. Philips Healthcare. [Online] 2004-2011. [Cited: May 25,
2011.] <http://www.healthcare.philips.com/main/>.

Protection of Humans available online at

Radiation: A summary of Judgments for the purposes of Radiological
Radiology Rounds A Newsletter for Referring Physicians

Massachusetts General Hospital Department of Radiology, volume 8 issue 3
march 2003.

Radiology. 2005;235:756–773.

Rehani M, Berry M. 2000 Radiation doses in computed tomography
(Editorial). Br. Med. J. 320, 593-594..

Rehani M, Computed tomography: Radiation dose considerations.
In: Advances in Medical Physics, M.M. Rehani (Ed), Jaypee Bros
Medical Publishers, N. Delhi, pp.125-133. 2000.

Seibert JA, Boone JM. X-ray imaging physics for nuclear medicine technologists part 2: x-ray interactions and image formation. J Nucl Med Technol. 2005;33:3–18.

Shrimpton, P.C., D.G. Jones, M.C. Hillier et al (1991). Survey of CT practice in the UK. Part Dosimetric aspects. NRPB-R249. NRPB, Chilton. Standardized Nomenclature and Description of CT Scanning Techniques.

Strategies for CT radiation dose optimization. Kalra, M. K., Maher, M. M., Toth, T. L., Hamberg, L. M., Blake, M. A., Shepard, J. A. and Saini, S. 203(3):619-628, s.l. : RSNA, March 2004, Radiology.

Thijsen MAO, Thijsen HOM, Mers JL, Lindeijer JM, Bijerk KR (1989) A definition of image quality: the image quality figure. BIR Rep 20:29–34 21. tube current control: principles and validation on phantoms and cadavers. Eur Radiol 9,323-328.1999.

United Nations Scientific Committee on the Effects of Atomic Radiation(2000). Report to the General Assembly, Annex D Medical Radiation Exposures. United Nations, New York.

Verdun FR, Moeckli R, Valley JF, Bochud F, Hessler C (1996) Survey on image quality and dose levels used in Europe for mammography. Br J Radiol 69:762–768

William R. Hendee and E. Russell Ritenour, Medical Imaging Physics, Fourth

Appendix (B)
Medical images

